Notes for C5.7: Topics in Fluids. MT 2024.

Contents

1 A Brief Refresher

1.1 The Navier-Stokes equations

The velocity field of a fluid of density ρ, viscosity μ satisfies the Navier–Stokes equations

$$\rho\frac{\mathrm{D}\mathbf{u}}{\mathrm{D}t} = -\nabla p + \mathbf{F} + \mu\nabla^2\mathbf{u}, \quad \frac{\mathrm{D}\rho}{\mathrm{D}t} + \rho\nabla\cdot\mathbf{u} = 0, \tag{1.1}$$

where p is the pressure and $\mathbf{F}$ is a body force (i.e. a force that acts on the whole body, not just at the surface; most often we shall have that $\mathbf{F} = \rho\mathbf{g}$, the force per unit volume due to gravity). The material derivative

$$\frac{\mathrm{D}}{\mathrm{D}t}() \equiv \left[\frac{\partial}{\partial t} + \mathbf{u}\cdot\nabla\right]().$$

The first of the equations in (1.1) comes from a consideration of the conservation of momentum, whilst the second comes from the conservation of mass. A detailed derivation is given in the appendix (and is not examinable).

If the typical flow speed is U, the length scale of the flow is L then a typical time scale is L/U. We would like to non-dimensionalize (1.1) but we need to choose a relevant pressure scale p^*. If we continue regardless and scale the body force with p^*/L then we find that

$$\frac{\mathrm{D}\mathbf{u}}{\mathrm{D}t} = \frac{p^*}{\rho U^2}\left(-\nabla p + \mathbf{F}\right) + \frac{1}{\mathrm{Re}}\nabla^2\mathbf{u} \tag{1.2}$$

where

$$\mathrm{Re} = \frac{\rho U L}{\mu} \tag{1.3}$$

is the *Reynolds number* and measures the relative importance of inertia and viscosity. One way to see this is to write

$$\mathrm{Re} = \frac{\rho U^2}{\mu U/L} = \frac{p^*_{inertia}}{p^*_{viscous}}$$

where $p^*_{inertia} = \rho U^2$ is the important pressure scale when the left hand side of (1.2) is important (i.e. when the inertia of the liquid is important) and $p^*_{viscous} = \mu U/L$ is the important pressure scale when the $\mathbf{u}$ dependence on the right hand side of (1.2) is important (i.e. when the viscosity of the liquid is important).

Boundary conditions   The Navier–Stokes equations in general require two boundary conditions to be applied either at a boundary either with another fluid (liquid or gas) or with a solid. The first of these conditions is the *no-slip boundary condition*, which states that the tangential component of the fluid's velocity must be the same as that of the boundary. Mathematically, this may be written

$$[\mathbf{u} \wedge \mathbf{n}]_-^+ = 0 \tag{1.4}$$

where $\mathbf{n}$ is the normal to the boundary and the notation $[f]_-^+$ means "*the change in $f(x)$ across the boundary*", i.e. $[f]_-^+ = \lim_{\epsilon \to 0} [f(0 + \epsilon) - f(0 - \epsilon)]$ for a problem with a boundary at $x = 0$.

The second boundary condition is the *kinematic boundary condition*, which states that the normal velocity to any boundary must be continuous across that boundary, i.e.

$$[\mathbf{u} \cdot \mathbf{n}]_-^+ = 0. \tag{1.5}$$

This is a direct consequence of the conservation of mass applied at a boundary.

When the boundary in question is a free surface, $z = f(x, y, t)$, it is common to use a corollary of the kinematic boundary condition that

$$w = f_t + \mathbf{u} \cdot \nabla f, \quad \text{on} \quad z = f(x, y, t) \tag{1.6}$$

or, equivalently, that

$$\frac{\mathrm{D}(z - f)}{\mathrm{D}t} = 0, \tag{1.7}$$

i.e. that particles that start on the surface remain on the surface.

Some simplifications   The dimensionless version of the Navier–Stokes equations, (1.2), suggests that (1.2) may simplify considerably in the limits of Re $\ll 1$ and Re $\gg 1$. We consider briefly these limits now.

1.1.1   Re $\ll 1$: Stokes flows

In the limit of Re $\ll 1$ we take $p^* = \mu U / L$ so that (1.2) becomes

$$\nabla^2 \mathbf{u} + \mathbf{F} = \nabla p. \tag{1.8}$$

Equation (1.8) is referred to as *Stokes' equation* and flows that satisfy this equation are known as *Stokes flows*.

1.1.2   Re $\gg 1$: Euler flows

In the limit of Re $\gg 1$ we take $p^* = \rho U^2$ so that (1.2) becomes

$$\frac{\mathrm{D}\mathbf{u}}{\mathrm{D}t} = \mathbf{F} - \nabla p. \tag{1.9}$$

Equation (1.9) is referred to as *Euler's equation* and is covered in detail in the Part A *Fluid Dynamics & Waves* course. Note that in Euler flows, the no-slip condition cannot be enforced (since the problem is only second order and hence can only have one boundary condition). In reality, the neglect of the $\nabla^2\mathbf{u}/\mathrm{Re}$ term leads to boundary layers where the viscosity of the liquid is important; the no-slip boundary condition is satisfied in the inner problem associated with the boundary layer.

1.1.3 The Boussinesq approximation

For some portions of this course we shall be interested in flows that are generated by changes in buoyancy, for example in the convection generated by heating a fluid from below. To simplify the analysis of such situations we shall make the following commonly used assumptions:

1. Changes in density caused by the onset of motion are primarily the result of temperature and composition (rather than pressure) changes.

2. In the equations expressing the conservation of momentum and mass, density changes may be neglected *except* where they are coupled to the gravitational acceleration in the buoyancy force.

Collectively, these assumptions are referred to as the *Boussinesq approximation*. A rational justification of these assumptions can be given in certain situations [see, for example, E. A. Spiegel & G. Veronis, *Astrophys. J.* **131**, 442 (1960)]. However, for the purposes of this course we shall simply make this assumption. In particular, we note that in this situation the conservation of mass simplifies to

$$\nabla\cdot\mathbf{u} = 0, \tag{1.10}$$

i.e. we assume that the flow is *incompressible*.

1.1.4 Two-dimensional flows

For flows in two dimensions, it is possible to ensure that the incompressibility condition (1.10) is automatically satisfied by expressing the velocity field $\mathbf{u}$ in terms of a *streamfunction ψ*. The details of doing this depend on the exact geometry in hand. The most useful cases are the following:

- *Planar flows.* In this case $\mathbf{u} = (u, v, 0)$ and we let

$$u = \frac{\partial\psi}{\partial y}, \quad v = -\frac{\partial\psi}{\partial x}.$$

- *Axisymmetric flows: Cylindrical Polars.* In this case $\mathbf{u} = (u_r, u_\theta, 0)$ and we let

$$u_r = \frac{1}{r}\frac{\partial\psi}{\partial\theta}, \quad u_\theta = -\frac{\partial\psi}{\partial r}.$$

- *Axisymmetric flows: Spherical Polars.* In this case $\mathbf{u} = (u_r, u_\theta, 0)$ and we let

$$u_r = \frac{1}{r^2\sin\theta}\frac{\partial\psi}{\partial\theta}, \quad u_\theta = -\frac{1}{r\sin\theta}\frac{\partial\psi}{\partial r}.$$

The relevant form of the streamfunction can be substituted into the relevant limit of (1.2), which may then be solved for the function ψ safe in the knowledge that the velocity field that results from the solution will be divergence free by construction.

1.2   Other Conservation Laws

The Navier–Stokes equations consist of a mathematical description of the conservation of mass and conservation of momentum, as we have already seen. In some of the situations considered in this course we will want to describe the conservation of other quantities, most notably the conservation of a solute (for example salt in sea water) or energy (for example convection due to differences in temperature). The conservation of a solute typically takes the form of the advection–diffusion equation for the concentration $C(\mathbf{x}, t)$

$$\frac{\mathrm{D}C}{\mathrm{D}t} = \kappa_C \nabla^2 C \tag{1.11}$$

for a solute diffusion coefficient κ_C. The conservation of energy may be complicated by the presence of a heat source q as well as the working of pressure forces in volume changes and describes the evolution of the temperature field $T(\mathbf{x}, t)$:

$$\rho c_v \frac{\mathrm{D}T}{\mathrm{D}t} = -p \boldsymbol{\nabla} \cdot \boldsymbol{u} + \boldsymbol{\nabla} \cdot (k \boldsymbol{\nabla} T) + \rho q. \tag{1.12}$$

where c_v is the specific heat at constant volume. However, this too will frequently reduce to an advection–diffusion equation (for Boussinesq flows with no internal heat generation) and so we have

$$\frac{\mathrm{D}T}{\mathrm{D}t} = \kappa_T \nabla^2 T, \tag{1.13}$$

where $\kappa_T = k/\rho c_v$ is the thermal diffusivity.

2   Surface Tension and Viscous Flows

2.1   Surface tension

2.1.1   What is surface tension?

Liquids consist of molecules tightly packed together and interacting with one another through an attractive force (this is why gases condense to form liquids when the molecules are slowed down by cooling). A molecule in the bulk of a liquid is therefore 'happy' in the sense that it feels these attractive interactions from all directions. A molecule at the liquid surface, however, is 'unhappy' because it has attractive interactions with only half as many neighbours as the bulk molecule. This unhappiness corresponds to an increase in the potential energy of the system and is why liquids like to minimize their surface area when free to do so. If the energy difference between the bulk and interfacial molecules is U then having molecules of cross-sectional area a^2 at the interface (rather than in the bulk) will cost U/a^2 per unit of the liquid's surface area. For many liquids the attractive interaction is caused by relatively weak van der Waals interaction and so we have that $U \approx k_B T$ — the thermal energy. At room temperature, $k_B T \approx 4 \times 10^{-21}$ J, and so for a molecule with typical 'radius' 0.1 nm we find that this surface energy is $\gamma \approx 0.1$ Nm^{-1}. For an air–water interface detailed measurements show that $\gamma = 72.8$ mJm^{-2} at room temperature. Other liquid–gas interfaces typically differ in the value of γ a little: the largest normal value is for an air–mercury interface, which has $\gamma = 485$ mJm^{-2}.
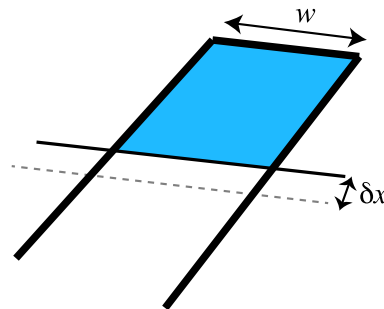
Figure 2.1: Thought experiment demonstrating that a surface energy γ can also be thought of as a surface 'tension'. A rod is free to move on a wire frame that makes a soap film. The decrease in surface energy $2\gamma w \delta x$ is equivalent to the work done by a force $F = 2\gamma w$ acting on the rod over a distance δx.

Note that the units of the surface energy γ are $[\gamma] = $ Jm$^{-2} = $ Nm^{-1}, which is also the units used to measure tensions. To see that the surface energy γ can also 'pull', just like the tension in a string, consider the following thought experiment: a soap film is formed within a rectangular frame with three rigid sides and one rigid rod that is free to move (see figure 2.1). In this situation, the energy of
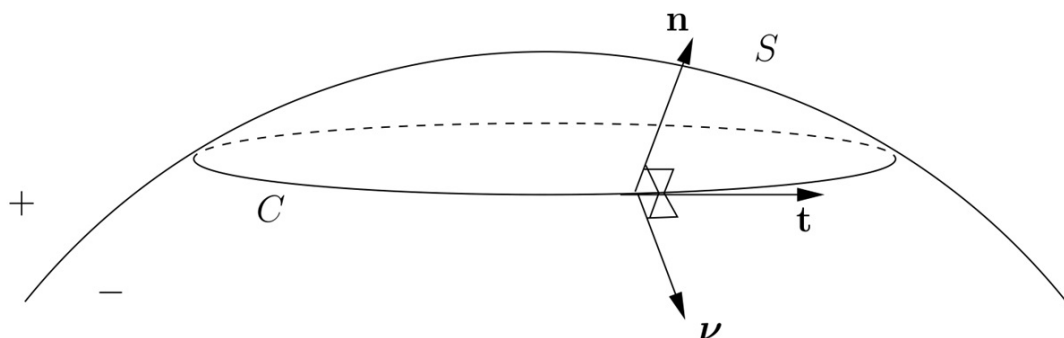
Figure 2.2: A small element of surface.

the system is reduced by moving the mobile rod. In moving a distance δx the surface energy of the system is decreased by an amount $2\gamma \cdot \delta x \cdot w$ where w is the width of the rectangle and the factor 2 arises because there are actually 2 liquid–gas interfaces in this scenario. Since energy is conserved in this system, the work done on the rod is $\delta W = 2\gamma w \delta x = F \delta x$: i.e. a force $F = 2\gamma w$ acts on the rod. There is thus a surface tension of magnitude γ that acts within the plane of the surface. How do we quantify its effect on the fluid below?

2.1.2   Stress conditions at a fluid-fluid interface

Consider an (arbitrarily small) section of an interfacial surface S bound by a closed contour C as shown in Figure 2.2. The force on S due to surface tension is exerted around the boundary C in a direction perpendicular to C but tangent to the surface S (call this direction $\boldsymbol{\nu}$) and is of magnitude γ per unit length.

Now consider a small volume element created by moving a distance $(-\epsilon, \epsilon)$ normal to S. A force balance on this element gives

$$\int_V \rho \frac{\mathrm{D}\mathbf{u}}{\mathrm{D}t} \, \mathrm{d}V = \int_V \mathbf{f} \, \mathrm{d}V + \int_S \left(\mathbf{t}^+ + \mathbf{t}^-\right) \, \mathrm{d}S + \int_C \gamma\boldsymbol{\nu} \, \mathrm{d}s,$$

where

- $\mathbf{f}$ is the body force
- $\mathbf{u}$ the fluid velocity
- ρ the fluid density
- $\mathbf{t}^+$ the force per unit area that the upper (+) fluid exerts on the top surface
- $\mathbf{t}^-$ the force per unit area that the lower (−) fluid exerts on the bottom surface.

Letting $\epsilon \to 0$ the volume integrals scale like ϵ and tend to zero. We conclude that the surface forces must be in balance, and hence that:

$$0 = \int_S \left(\mathbf{t}^+ + \mathbf{t}^- \right) \, \mathrm{d}S + \int_C \gamma \boldsymbol{\nu} \, \mathrm{d}s.$$

Now, if the stress tensor in the fluid is

$$\mathbf{T} = -p\mathbf{I} + \mu \left[\nabla \mathbf{u} + (\nabla \mathbf{u})^T \right],$$

where p is the pressure and μ is the viscosity, then the surface forces per unit area are

$$\mathbf{t}^+ = \mathbf{n} \cdot \mathbf{T}^+, \qquad \mathbf{t}^- = -\mathbf{n} \cdot \mathbf{T}^-,$$

where $\mathbf{n}$ is the unit upward normal to S (from $-$ to $+$).

Defining γ and $\mathbf{n}$ off surface by an extension which is invariant in the direction perpendicular to the tangent plane, we find that Stokes Theorem (see Problem Sheet 1) gives

$$\int_C \gamma \boldsymbol{\nu} \, ds = \int_S \left[\nabla \gamma - \gamma (\nabla \cdot \mathbf{n}) \, \mathbf{n} \right] \, dS.$$

With

$$\nabla_s = \nabla - \mathbf{n} \frac{\partial}{\partial n}$$

denoting the surface gradient, and noting with the above definition of γ and $\mathbf{n}$ off surface, we have $\nabla \gamma = \nabla_s \gamma$ and $\nabla \cdot \mathbf{n} = \nabla_s \cdot \mathbf{n}$ and hence

$$\int_C \gamma \boldsymbol{\nu} \, ds = \int_S \left(\nabla_s \gamma - \gamma \nabla \cdot \mathbf{n} \, \mathbf{n} \right) \, dS.$$

Thus

$$\int_S \left(\mathbf{n} \cdot \mathbf{T}^+ - \mathbf{n} \cdot \mathbf{T}^- \right) \, dS = \int_S \left[\gamma (\nabla \cdot \mathbf{n}) \, \mathbf{n} - \nabla_s \gamma \right] \, dS.$$

Since the surface element S was arbitrary, the integrand must vanish identically, giving the interface force balance equation

$$\mathbf{n} \cdot \mathbf{T}^+ - \mathbf{n} \cdot \mathbf{T}^- = \gamma (\nabla \cdot \mathbf{n}) \, \mathbf{n} - \nabla_s \gamma. \tag{2.1}$$

The left-hand side of this equation is the difference between the force per unit area exerted on the interface by the upper and lower fluids. The first term on the right-hand side is a normal force per unit area generated by the curvature of the surface (see next section). The second term on the right-hand side is a tangential force per unit area associated with gradients in surface tension.

Equation (2.1) is a vector equation, which is often written in terms of its normal and tangential components. Taking the inner product with $\mathbf{n}$ gives the normal force balance

$$\mathbf{n} \cdot \mathbf{T}^+ \cdot \mathbf{n} - \mathbf{n} \cdot \mathbf{T}^- \cdot \mathbf{n} = \gamma (\nabla \cdot \mathbf{n}). \tag{2.2}$$
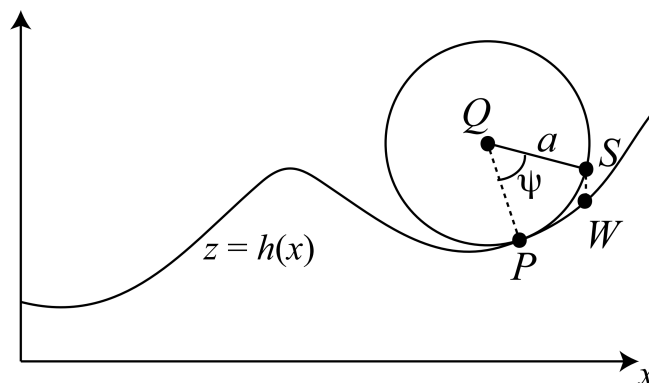
Figure 2.3: Setup diagram for the determination of the radius of curvature, a.

Taking the inner product with any tangent vector $\mathbf{t}$ gives the tangential force balance

$$\mathbf{n} \cdot \mathbf{T}^+ \cdot \mathbf{t} - \mathbf{n} \cdot \mathbf{T}^- \cdot \mathbf{t} = -\nabla_s \gamma \cdot \mathbf{t}. \tag{2.3}$$

2.1.3   Curvature

Curvature in two dimensions See Appendix for more details. The magnitude of the curvature of a 2D surface at a point P is the reciprocal of the radius of the best fit circle to the surface at P. We seek an expression for the curvature in terms of the unit normal at P. A detailed derivation of the 2D result is given in the appendix (and is not examinable).

Defining the 2D surface by $z = h(x)$, we first find the unit normal and unit tangent vectors:

$$\mathbf{n} = \frac{(-h', 1)}{(1 + h'^2)^{1/2}}, \qquad \mathbf{t} = \frac{(1, h')}{(1 + h'_2)^{1/2}}.$$

Then the magnitude of the curvature at P is given by

$$\frac{1}{a} = \frac{h_0''}{(1 + h_0'^2)^{3/2}} = -\nabla \cdot \mathbf{n}_0.$$

More generally, the magnitude of the curvature at the point x is given by

$$\left| \frac{h''(x)}{(1 + h'(x)^2)^{3/2}} \right| = |\nabla \cdot \mathbf{n}|$$

and the curvature, κ, is *defined* by

$$\kappa = -\nabla \cdot \mathbf{n}.$$

Thus the curvature is positive if the centre of curvature lies above the surface and negative if it is below (with the contrast between above and below determined by the direction of the unit normal).

Curvature in three dimensions In three dimensions let $z = h(x, y)$ denote a surface and consider the point

$$(x_p, y_p, h(x_p, y_p)).$$

With x_P, y_P fixed and λ constant the line

$$y - y_p = \lambda(x - x_p)$$

defines a two dimensional surface via

$$z = h(x, y_p + \lambda(x - x_p)).$$

Its curvature at $x = x_p$ can be found as above and varies with λ. The sum of the maximum of these curvatures and the minimum of these curvatures defines the **total** curvature, denoted κ, at the point P. With the normal

$$\mathbf{n} = \frac{1}{\left| \nabla(z - h(x, y)) \right|} \nabla(z - h(x, y)),$$

defined off-surface by an extension which is independent of the direction perpendicular to the tangent plane, so that

$$-\nabla \cdot \mathbf{n} = \frac{h_{xx}(1 + h_y^2) + h_{yy}(1 + h_x^2) - 2h_x h_y h_{xy}}{(1 + h_x^2 + h_y^2)^{3/2}},$$

the total curvature is equal to

$$\kappa = -\nabla \cdot \mathbf{n}.$$

We do not prove this statement here (see e.g. Weatherburn, C. E., 1961, Differential Geometry of Three Dimensions, Vol. 1, C.U.P.).

2.1.4 Capillary statics

We consider here static fluid configurations, for which $\mathbf{u} = \mathbf{0}$. The stress tensor in the fluid is then $\mathbf{T} = -p\,\mathbf{I}$, so that

$$\mathbf{n} \cdot \mathbf{T} \cdot \mathbf{n} = -p, \qquad \mathbf{n} \cdot \mathbf{T} \cdot \mathbf{t} = 0.$$

The normal stress boundary condition is then

$$p^+ - p^- = \gamma \kappa.$$

There is a pressure jump across the interface which is balanced by the force due to curvature. The tangential stress boundary condition is

$$\mathbf{0} = -\nabla_s \gamma.$$

Thus we see that there cannot be a static system in the presence of surface tension gradients. Pressure jumps can sustain normal stress jumps across a fluid interface, but they do not contribute to the tangential stress. Thus tangential surface stresses can only be balanced by the viscous stresses associated with fluid motion.

Stationary bubble

Consider a spherical bubble of radius R submerged in a stationary fluid. The curvature of the spherical interface is

$$-\kappa = \nabla \cdot \mathbf{n} = \nabla \cdot \left(\frac{\mathbf{r}}{r}\right) = \frac{1}{r^2}\frac{\partial}{\partial r}\left(r^2\right) = \frac{2}{R}.$$

Thus the normal force balance gives

$$p^- - p^+ = \frac{2\gamma}{R}.$$

The pressure within the bubble, p^-, is higher than that outside by an amount proportional to the surface tension, and inversely proportional to bubble radius. Small bubbles have a higher internal pressure, and are consequently louder than large bubbles when they burst at a free surface: champagne is louder than beer.

Note that soap bubbles in air have two free surfaces (the inner and outer surfaces of the soap film). Consequently the pressure difference between the inside and outside of the bubble is twice that across a single interface.

Static meniscus

Consider a situation in which a heavy fluid such as water lies stationary below a much lighter fluid such as air. The pressure in the air is constant, so that $p^+ = p_0$ say, but the pressure in the water varies due to the presence of gravity, so that

$$p^- = p_0 - \rho g z,$$

where p_0 is constant, z is the vertical coordinate, and $\boldsymbol{g} = -g\boldsymbol{e}_z$ is the gravitational acceleration. The normal force balance on the interface now gives

$$\rho g z = \gamma \kappa. \tag{2.4}$$

Equation (2.4) is known as the *Laplace–Young equation.*

Consider the planar meniscus that arises where the air-water interface meets the wall of a container, as shown in Figure 2.4. If we define the free surface to be given by $z = h(x)$ then its curvature is

$$\kappa = \frac{h_{xx}}{(1 + h_x^2)^{3/2}}. \tag{2.5}$$

The Laplace–Young equation for the interface shape may therefore be written

$$\rho g h = \gamma \frac{h_{xx}}{(1 + h_x^2)^{3/2}}. \tag{2.6}$$

in this instance. Since this is a second-order differential equation we require two boundary conditions for its solution. Requiring that $h \to 0$ as $x \to \infty$ provides one of these conditions. However, we need
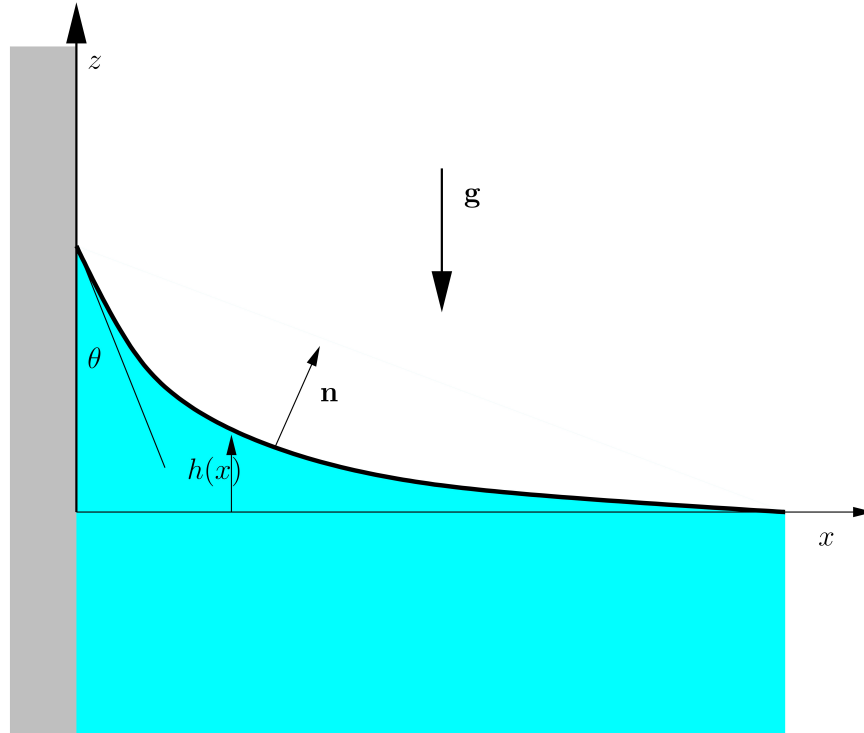
Figure 2.4: A meniscus. The shared interface among the three phases of the solid, liquid and gas is known as a *contact line*; here the contact line is perpendicular to the page and is simply a point in the figure (the vertex of the arc subtended by θ). More generally a contact line refers to the shared interface of a solid and two different fluids.

another condition at $x = 0$. Based on experimental observations, we postulate that the angle between the air–water interface and the immersed boundary is a constant that depends on the nature of the three phases (liquid, solid and gas) that meet at $x = 0$. This 'contact angle' θ depends on the physics of the interaction between the wall and the air and water (in particular on how easy it is for the water to "wet" the wall). We will return to contact angles later, but for now we treat θ as an experimentally determined constant.

If θ is close to $\pi/2$, the slope of the meniscus remains small ($h_x \ll 1$) and we can linearise (2.6) to give

$$\rho g h = \gamma h_{xx},$$

with the boundary conditions

$$h(\infty) = 0, \qquad h_x(0) = -\cot\theta.$$

Thus

$$h = \ell_c \cot\theta \, e^{-x/\ell_c}, \tag{2.7}$$

where $\ell_c = \sqrt{\gamma/\rho g}$ is the *capillary length*. Thus the meniscus is a decaying exponential, with a decay
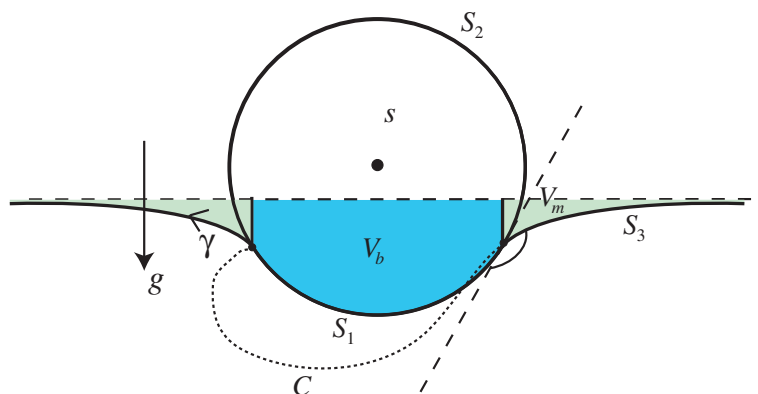
Figure 2.5: The volumes displaced by a floating two-dimensional object: V_b is the volume displaced by the object itself, V_m the volume displaced by the associated meniscus. Note that the contact line C is drawn coming out of the page.

length of ℓ_c. For an air–water interface, $\ell_c \approx 3$ mm explaining why the meniscus is only observed very close to the edge in a glass of water.

Floating bodies

Floating bodies are supported by a combination of buoyancy and surface tension forces. Consider a two-dimensional non-wetting body. Then the pressure in the fluid is

$$p = p_0 - \rho g z$$

so that the pressure at the interface $z = h(x)$ is

$$p = p_0 - \rho g h.$$

Let $\mathbf{n}$ denote the unit inward normal to the body with the part of the body in contact with the water labelled by S_1. The part of the body in contact with the air is S_2, and the *contact line*, C, is the wetting curve separating the air from the liquid on the body (drawn out of the page in figure 2.5). Then the force on the body is

$$\int_{S_1} p\mathbf{n} \ \mathrm{d}S + \int_{S_2} p_0\mathbf{n} \ \mathrm{d}S + \int_C \gamma\boldsymbol{\nu} \ \mathrm{d}s \ = \ \int_{S_1 \cup S_2} p_0\mathbf{n} \ \mathrm{d}S - \int_{S_1} \rho g h\mathbf{n} \ \mathrm{d}S + \int_{S_1} \gamma\kappa\,\mathbf{n} \ \mathrm{d}S$$

noting that $\nabla_s\gamma = 0$ as $\mathbf{u} = 0$. Using the facts that p_0 is constant and that

$$\int_S \mathbf{n} \ \mathrm{d}S = 0$$

(which may be proved by applying the divergence theorem to the above integral after dotting with an arbitrary constant vector), the force on the body simplifies to

$$-\int_{S_1} \rho g h \mathbf{n} \ \mathrm{d}S + \int_{S_1} \gamma \kappa \, \mathbf{n} \ \mathrm{d}S.$$

Thus the vertical force balance is

$$M g = \boldsymbol{e}_z \cdot \int_{S_1} (-\rho g h + \gamma \kappa) \, \mathbf{n} \ \mathrm{d}S = F_b + F_c,$$

say. The buoyancy force

$$F_b = -\boldsymbol{e}_z \cdot \int_{S_1} \rho g h \, \mathbf{n} \ \mathrm{d}S = \rho g V_b$$

is simply the weight of the fluid above the object and inside the line of tangency (see figure 2.5).

The surface tension forces

$$F_c = \boldsymbol{e}_z \cdot \int_{S_1} \gamma \kappa \mathbf{n} \ \mathrm{d}S,$$

may be re-written using the Laplace–Young equation on the free surface. First, by Stokes theorem we have

$$\int_{S_1} \gamma \kappa \mathbf{n} \ \mathrm{d}S + \int_{S_3} \gamma \kappa \mathbf{n} \ \mathrm{d}S = \int_{C_\infty} \gamma \boldsymbol{\nu} \ \mathrm{d}s = \gamma \int_{C_\infty} \boldsymbol{\nu} \ \mathrm{d}s.$$

Here S_3 is the free surface (with outward pointing normal $\mathbf{n}$) and C_∞ is an arbitrarily large circular contour bounding the meniscus; we have used the fact γ is constant as the fluid is static. On C_∞ the fluid is essentially flat; the deviations of the unit normal from $\hat{\boldsymbol{e}}_z$ are exponentially small and thus convergence to flatness is sufficiently fast. Thus $\boldsymbol{\nu} = \mathbf{e}_r$ to within exponentially small errors in the distance from the body and hence the above integral tends to zero as the distance from the body tends to infinity, giving

$$\int_{S_1} \gamma \kappa \mathbf{n} \ \mathrm{d}S = -\int_{S_3} \gamma \kappa \mathbf{n} \ \mathrm{d}S.$$

Hence

$$\boldsymbol{e}_z \cdot \int_C \gamma \boldsymbol{\nu} \ \mathrm{d}s = \mathbf{z} \cdot \int_{S_1} \gamma \kappa \mathbf{n} \ \mathrm{d}S = -\boldsymbol{e}_z \cdot \int_{S_3} \gamma \kappa \mathbf{n} \ \mathrm{d}S,$$

But on the free surface, S_3, buoyancy and surface tension exactly balance and hence the Laplace-Young equation holds, giving

$$\rho g h = \gamma \kappa.$$

Thus

$$F_c = -\boldsymbol{e}_z \cdot \int_{S_3} \rho g h \mathbf{n} \ \mathrm{d}S = \rho g V_m,$$

where V_m is the volume of fluid displaced above the meniscus outside the line of tangency. Thus the total upward force on the body may be expressed as

$$\rho g (V_b + V_m).$$

This is the generalization of Archimedes' principle to incorporate the vertical force from surface tension. More details may be found in a paper by Keller, *Phys. Fluids* **10**, 3009 (1998).

To consider the relative sizes of the contributions from the conventional Archimedes force and that due to surface tension, we note that the meniscus will have a length comparable to the capillary length ℓ_c, so that

$$V_b \sim \text{depth} \times R^2, \qquad V_m \sim \text{depth} \times R\ell_c,$$

where R is a typical lengthscale of the body. Thus the relative magnitude of buoyancy and capillary forces is

$$\frac{F_b}{F_c} \approx \frac{R}{\ell_c};$$

very small floating objects ($R \ll \ell_c$) are principally supported by surface tension forces. This explains why small, dense objects such as drawing pins are able to float at the surface of water despite being many times denser than the water (see figure 2.6a) as well as how small creatures are able to walk on the surface of liquids (figure 2.6b).
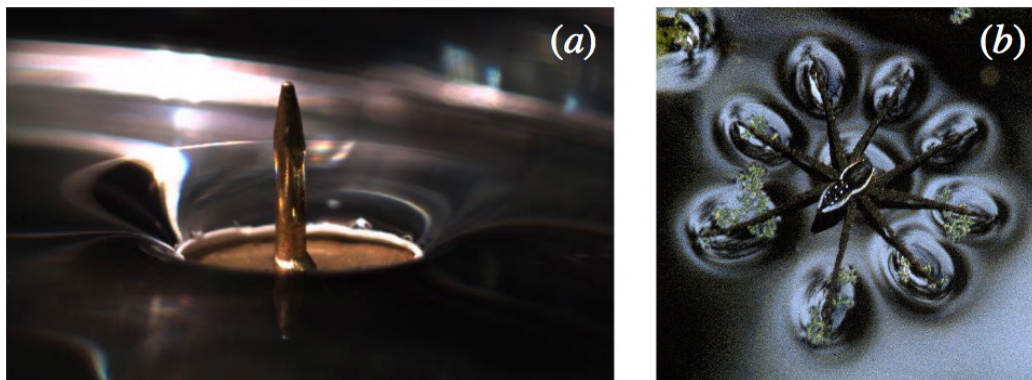
Figure 2.6: The large deformations produced by interfacial objects. (a) The vertical component of surface tension is sufficient to balance the weight of objects much denser than the underlying liquid, such as an upturned drawing pin floating on water. (b) Large interfacial deformations allow creatures such as the fishing spider (*Dolomedes triton*) to walk on water (image courtesy of Robert B. Suter of Vassar College).

End lecture 1

2.1.5   Marangoni flows

Marangoni flows are those driven by surface tension gradients. In general the surface tension γ depends on both the temperature, T, and the concentration, C, of interfacial contaminants. As the temperature of a liquid increases, the surface tension coefficient generally decreases. For an air–water interface, $\gamma^{-1} \, \mathrm{d}\gamma/ \, \mathrm{d}T \approx -1/50\mathrm{K}$. Surface active agents ('surfactants') contain a hydrophobic tail (non-polar) and a hydrophilic head (polar) and so like to reside at the air–liquid interface. The presence of these surfactant molecules *decreases* the surface tension coefficient.

Tears of wine

The tears of wine phenomenon was the first Marangoni flow to be considered (by Lord Kelvin in 1885), and predates Marangoni's first published work on the subject by a decade.

Tears of wine can be easily observed in all but the weakest wines after swishing the glass to establish a thin layer of fluid on the walls. Evaporation of alcohol occurs everywhere along the free surface. The alcohol concentration in the thin layer is thus reduced by comparison to the bulk due to the enhanced surface to volume ratio. Surface tension decreases with alcohol concentration, so that the surface tension in the film is higher than that in the bulk. The resulting surface tension gradient acts to drive fluid up the film. The wine climbs until it reaches the top of the film, where it collects in a band of fluid that thickens until eventually becoming unstable due to gravity and releasing the tears of wine. The tears or 'legs' roll down to replenish the bulk reservoir, but with fluid that is depleted with alcohol.

Surfactants

Surfactants alter both the normal (through the reduction of γ) and tangential (through the generation of marangoni forces) stress balances. The presence of surfactants will act to supress any fluid motion characterised by a nonzero surface divergence. For example, consider a fluid motion characterised by a radially divergent surface motion. The expansion of the surface means that Γ is reduced near the point of divergence, increasing the surface tension there. The resulting Marangoni stresses act to reduce the surface motion. Similarly if the flow is characterised by a radial convergence, the resulting accumulation of surfactant in the region of convergence will decrease the surface tension again generating marangoni forces which oppose the flow. This is one reason why soap films survive as long as they do: the divergent motions that would cause a pure liquid film to rupture are suppressed by the surfactant layer on the soap film surface.

The ability of surfactant to suppress flows with non-zero surface divergence is behind the phrase "pouring oil on troubled waters," and is evident throughout nature. It was remarked upon by Pliny the Elder, who rationalised that the absence of capillary waves in the wake of ships is due to them stirring up surfactant. It is also responsible for the "footprints of whales". In the wake of whales one sees patches on the sea surface (of characteristic width 5-10m) that are perfectly flat. These are generally acknowledged to result from whales sweeping biomaterial to the surface with their tails; this biomaterial acts as a surfactant to suppress capillary waves.

Effect of surfactants on bubble motion

Theoretical predictions for the rise speed of small bubbles do not adequately describe experimental observations. Air bubbles rise at low Reynolds numbers at rates more appropriate for rigid spheres with equivalent buoyancy in all but the most carefully cleaned fluids. The discrepancy can be explained by considering the effect of surfactants.

The flow around a bubble diverges and converges at the leading and trailing surfaces respectively. In the presence of surfactant contamination surfactants will accumulate at the trailing edge, giving rise to a local decrease in surface tension. The resulting surface tension gradient acts to resist surface

motion, so that the bubble surface is more rigid. The air bubble thus moves as if its surface were fixed, so that its rise rate is closer to that of a rigid sphere: the no-slip boundary condition is more appropriate than free-slip. The effect is more pronounced for small bubbles, since the Marangoni force scales as $\Delta\gamma/R$, where R is the bubble radius.

Thermo-capillary bubble motion

Analogously to the 'rigidification' of the bubble's surface described above, a bubble placed in a temperature gradient can move because of the Marangoni stresses induced by the temperature gradient. This was used by Young *et al.* (*J. Fluid Mech.* **6**, 350 (1959)) to counteract the buoyancy-induced rise of a bubble. We now present a calculation that quantifies this 'thermo-capillary' motion. For simplicity, we shall assume that the bubble remains spherical as it moves, though in fact it is possible to show *a posteriori* that tho is the case provided that the bubble motion occurs at low Reynolds number.

We imagine that the temperature field is imposed everywhere (including within the bubble) to be

$$T = T_\infty + T'z \tag{2.8}$$

in the frame moving with the bubble. (Note that temperature field satisfies $\nabla^2 T = 0$ and so relies on the convection of heat being negligible compared with its diffusion. We are also implicitly assuming that the bubble and fluid have the same thermal conductivity.) We shall also assume that the relationship between surface tension coefficient and temperature is linear so that we may write the surface tension coefficient around the droplet as

$$\gamma = \gamma_0 + \gamma' z = \gamma_0 + \gamma' a \cos\theta. \tag{2.9}$$

We need to solve for the velocity field $\mathbf{u} = (u_r, u_\theta)$. Standard methods for Stokes flow (see §3.3 of Ockendon & Ockendon, Viscous Flow, for example) show that the velocity components are

$$u_r = \frac{1}{r^2 \sin\theta} \frac{\partial\psi}{\partial\theta}, \quad u_\theta = -\frac{1}{r\sin\theta} \frac{\partial\psi}{\partial r} \tag{2.10}$$

where the streamfunction ψ has the form

$$\psi = (Ar^4 + Br^2 + Cr + D/r) \sin^2\theta \tag{2.11}$$

in the spherical geometry of interest here. The coefficients A, B, C and D are to be determined by relevant boundary conditions. At $r = a$ we use the fact that the normal component of the fluid velocity must vanish on the sphere surface, i.e.

$$u_r(r = a) = 0 \tag{2.12}$$

and that the tangential shear stress is matched by that due to the temperature gradient

$$\tau_{r\theta} = \mu \left[r\frac{\partial}{\partial r}\left(\frac{u_\theta}{r}\right) + \frac{1}{r}\frac{\partial u_r}{\partial\theta} \right]_{r=a} = -\frac{1}{a}\frac{\partial\gamma}{\partial\theta} = \gamma' \sin\theta. \tag{2.13}$$

We also require that as $r \to \infty$ the velocity field returns to a uniform flow in the z-direction. This corresponds to

$$\psi \sim -\frac{U}{2}r^2 \sin^2 \theta, \quad r \to \infty. \tag{2.14}$$

We therefore have immediately that $A = 0$ and $B = -U/2$. From the requirement that $u_r(r = a) = 0$ we find that

$$C + D/a^2 = Ua/2, \tag{2.15}$$

while the tangential stress condition gives

$$D = -\frac{1}{6}\frac{\gamma' a^4}{\mu}. \tag{2.16}$$

Hence

$$C = \frac{Ua}{2} + \frac{1}{6}\frac{\gamma' a^2}{\mu}. \tag{2.17}$$

Finally we note that when a bubble is moving at its steady velocity and at low Reynolds number, the normal stress difference across the bubble surface is constant and equal to the pressure difference due to surface tension. Thus the difference in stresses does not act to deform the bubble away from its spherical shape and our assumption of a spherical bubble is justified. More details of this can be found in the book by Batchelor, page 238.

2.2   Thin Film Flows and the Lubrication Approximation

2.2.1   The lubrication approximation

Let us suppose we have a thin film of fluid with either a hard wall or a vacuum outside it. The typical thickness of the thin film will be denoted by H and the typical length over which variations in thickness occur will be L. We shall assume that $\delta = H/L \ll 1$.

We start with the incompressible Navier-Stokes equations

$$\rho\left(\mathbf{u}_t + \mathbf{u}\cdot\nabla\mathbf{u}\right) = -\nabla p + \rho\,\mathbf{g} + \mu\nabla^2\mathbf{u},$$

$$\nabla\cdot\mathbf{u} = 0.$$

where $\mathbf{g}$ is the gravitational acceleration.

Working in Cartesian co-ordinates (x, z) we shall assume that gradients satisfy

$$\frac{\partial}{\partial z} \sim 1/H \gg 1/L \sim \frac{\partial}{\partial x}$$

and so incompressibility $\nabla\cdot\mathbf{u} = 0$ gives us that the vertical velocity scale W is related to the horizontal velocity scale U by

$$W \sim HU/L = \delta U.$$

We may then consider the size of the terms in the horizontal component of the equation expressing conservation of momentum. We have

$$\rho(\mathbf{u}\cdot\nabla)u \sim \rho U^2/L, \quad \nabla p \sim p/L, \quad \mu\nabla^2 u \sim \mu U/H^2\left[1 + O(\delta^2)\right].$$

It is therefore clear that inertia may be neglected provided that

$$\frac{\rho U H}{\mu}\frac{H}{L} \ll 1. \tag{2.18}$$

Note that this condition involves the Reynolds number based on the film thickness modified by an additional factor δ. Note that this Reynolds number is often referred to as the *Reduced Reynolds number*. Inertia may therefore be neglected because of the thin geometry, even in situations where the gap Reynolds number itself is *not* that small. We also see that the natural scale for pressure in these systems is $p \sim \mu U L/H^2$.

Considering now the vertical component of the momentum equation, we have

$$\rho(\mathbf{u}\cdot\nabla)w \sim \rho U W/L \sim \delta\rho U^2/L, \quad \nabla p \sim p/H \sim \mu U L/H^3, \quad \mu\nabla^2 w \sim \mu\delta U/H^2 \sim \delta^2\nabla p$$

and so at leading order

$$\frac{\partial p}{\partial z} = \rho\mathbf{g}\cdot\boldsymbol{e}_z$$

so that the pressure is approximately hydrostatic. Furthermore, the flow is quasi-parallel to the boundary — we can neglect the vertical velocity to leading order.

End lecture 2

We must also consider the boundary conditions to be applied to the velocity field. At a fixed boundary we have the no slip condition
$$\mathbf{u} = 0.$$
At a free boundary $z = f(x, t)$ and we have the kinematic boundary condition
$$f_t + u f_x - w = 0. \tag{2.19}$$
We also have the stress balance equations (2.2), (2.3). The stress tensor is
$$\mathbf{T} = \begin{pmatrix} -p + 2\mu u_x & \mu(u_z + w_x) \\ \mu(u_z + w_x) & -p + 2\mu w_z \end{pmatrix},$$
while the normal and tangent to the surface are
$$\mathbf{n} = \frac{(-f_x, 1)}{(1 + f_x^2)^{1/2}}, \qquad \mathbf{t} = \frac{(1, f_x)}{(1 + f_x^2)^{1/2}},$$
and the curvature is
$$\kappa = \frac{f_{xx}}{(1 + f_x^2)^{3/2}}.$$
Thus the full free-surface stress boundary conditions are
$$-p + \frac{2\mu}{(1 + f_x^2)} \left(f_x^2 u_x - f_x(u_z + w_x) + w_z \right) = \frac{\gamma f_{xx}}{(1 + f_x^2)^{3/2}}, \tag{2.20}$$

$$2f_x(u_x - w_z) + (f_x^2 - 1)(u_z + w_x) = 0. \tag{2.21}$$

However, in keeping with our assumption that $\delta = H/L \ll 1$ and the consequences of this assumption that we have already explored, we find that the second term on the LHS of (2.20) is negligible and so (2.20) simplifies to
$$-p \approx \gamma f_{xx}. \tag{2.22}$$
Similarly, (2.21) simplifies considerably to yield
$$\frac{\partial u}{\partial z} = 0. \tag{2.23}$$

We can derive an integrated version of conservation of mass which is applicable in general. Let us suppose that the bottom surface is given by $Z = k(x, t)$ and the top surface is given by $Z = h(x, t)$. A key point to note is that the kinematic condition (2.19) also holds at a fixed surface (since $h_t = u = W = 0$ at a fixed surface).

$$
\begin{aligned}
\frac{\partial}{\partial x} \int_k^h u \, dZ &= \int_k^h \frac{\partial u}{\partial x} \, dZ + u(h, t) h_x - u(k, t) k_x \\
&= -\int_k^h \frac{\partial W}{\partial Z} \, dZ + u(h, t) h_x - u(k, t) k_x \\
&= W(k, t) - W(h, t) + u(h, t) h_x - u(k, t) k_x \\
&= k_t - h_t
\end{aligned}
$$

Thus, if we define the thickness of the film $\mathcal{H}$ and average velocity $\bar{u}$ by

$$\mathcal{H} = h - k, \qquad \bar{u} = \frac{1}{\mathcal{H}} \int_k^h u \, dZ,$$

then

$$\mathcal{H}_t + (\mathcal{H}\bar{u})_x = 0. \tag{2.24}$$

To complete the model we need to find an expression for the average velocity $\bar{u}$ in terms of $\mathcal{H}$. The details of this depend on the problem being considered. We now consider some examples.

2.2.2   Free surface flow down an inclined plane

Consider a thin film flowing down a plane inclined at an angle α to the horizontal. The direction of gravity in coordinates tangential and normal to the plane is given by

$$\hat{\mathbf{g}} = (\sin\alpha, -\cos\alpha).$$

The shape of the free surface $z = h(x, t)$ is unknown and must be determined. The fluid therefore lies between a fixed bottom surface $z = 0$ and a free top surface $z = h$. The pressure is determined by the vertical component of the momentum equation

$$\frac{\partial p}{\partial z} = -\rho g \cos\alpha$$

subject to the boundary condition (2.22). We find that

$$p = -\gamma h_{xx} + \rho g (h - z)\cos\alpha.$$

Substituting this expression into the horizontal momentum equation, we have

$$\mu \frac{\partial^2 u}{\partial z^2} = \frac{\partial p}{\partial x} - \rho g \sin\alpha = -\gamma h_{xxx} + \rho g \cos\alpha \, h_x - \rho g \sin\alpha. \tag{2.25}$$

Now for non-zero α and sufficiently shallow flows $h_x \ll \tan\alpha$ and so we may simplify this to find

$$\mu \frac{\partial^2 u}{\partial z^2} = -\gamma h_{xxx} - \rho g \sin\alpha. \tag{2.26}$$

We non-dimensionalize (2.26) using a velocity scale U and a length scale R to find

$$\frac{\partial^2 u}{\partial z^2} = -\frac{1}{\mathrm{Ca}} h_{xxx} - \frac{\mathrm{Bo}}{\mathrm{Ca}} \sin\alpha \tag{2.27}$$

where

$$\mathrm{Ca} \equiv \frac{\mu U}{\gamma} \tag{2.28}$$

measures the strength of viscous forces compared to capillary forces and is referred to as the *Capillary number* while

$$\text{Bo} \equiv \frac{\rho g R^2}{\gamma} \tag{2.29}$$

measures the relative strength of gravity to capillary forces and is referred to as the *Bond number*.

Integrating (2.26) subject to $u(0) = 0$ and $u_z(h) = 0$ we have

$$u = -\frac{z(z - 2h)}{2\text{Ca}} \left(h_{xxx} + \text{Bo} \sin \alpha \right)$$

so that the thickness-averaged velocity is

$$\bar{u} = \frac{h^2}{3\text{Ca}} \left(h_{xxx} + \text{Bo} \sin \alpha \right).$$

Substituting into (2.24) gives

$$h_t + \left[\frac{h^3}{3\text{Ca}} \left(h_{xxx} + \text{Bo} \sin \alpha \right) \right]_x = 0. \tag{2.30}$$

2.2.3 Free surface flow on a horizontal plane

Let us consider now that $\alpha = 0$ and that the fluid lies between a fixed bottom surface $Z = 0$ and a free top surface $Z = h$. Returning to (2.25) we see that our neglect of the h_x term in comparison to $\tan \alpha$ is no longer justified and so we now write

$$\mu \frac{\partial^2 u}{\partial z^2} = -\gamma h_{xxx} + \rho g h_x,$$

which may be solved to give, in dimensionless form,

$$u = -\frac{z(z - 2h)}{2\text{Ca}} \left(h_{xxx} - \text{Bo } h_x \right)$$

and hence

$$\bar{u} = \frac{h^2}{3\text{Ca}} \left(h_{xxx} - \text{Bo } h_x \right).$$

Finally, (2.24) gives

$$h_t + \left[\frac{h^3}{3\text{Ca}} \left(h_{xxx} - \text{Bo } h_x \right) \right]_x = 0. \tag{2.31}$$

2.2.4 Static solutions and the contact angle

Static meniscus against a vertical wall

See Fig. 2.4. Consider an infinite thin film of fluid which meets a vertical wall at $x = 0$, with contact angle θ; the thin film approximation requires the contact angle with the wall to be almost $\pi/2$. Thus

$$h_x(0) = -\cot \theta \approx \theta - \frac{\pi}{2}.$$

Suppose the height of the fluid at infinity is h_0; noting that h_x and h_{xxx} tend to zero at infinity we have

$$\left(\frac{h^3}{3\mathrm{Ca}} \left(h_{xxx} - \mathrm{Bo}\ h_x \right) \right)_x = 0$$

and hence $\dfrac{h^3}{3\mathrm{Ca}} \left(h_{xxx} - \mathrm{Bo}\ h_x \right) = \text{const.} = 0,$

using the condition at ∞ to set the integration constant to zero.

It is easy to see that the general solution is $h = a + be^{x/\ell_c} + ce^{-x/\ell_c}$, where $\ell_c = \sqrt{1/\mathrm{Bo}} = (\gamma/\rho g)^{1/2}/R$ is the dimensionless capillary length. The condition at infinity implies $a = h_0$, $b = 0$, while the condition at the origin gives $c = \ell_c\theta$. Hence

$$h - h_0 = \ell_c \left(\frac{\pi}{2} - \theta \right) e^{-x/\ell_c},$$

which is of course the same as (2.7) when θ is close to $\pi/2$.

Finite fluid drop lying on a horizontal plate

Figure 2.7: The definition of the contact angle θ

Consider a static drop of fluid, of total cross sectional area A. At a point where the film thickness goes to zero the contact angle is given. Thus if $h(x_0) = 0$ then

$$h_x(x_0) = \pm\tan\theta \approx \pm\theta.$$

This assumes that the contact angle is small (otherwise the lubrication approximation is violated near the contact line).

We suppose that the drop is symmetric about $x = 0$ and occupies the region $(-x_0, x_0)$, so that

$$
\begin{aligned}
h_x(0) &= 0, & \text{(2.32)} \\
h(x_0) &= 0, & \text{(2.33)} \\
h_x(x_0) &= -\theta, & \text{(2.34)} \\
\int_0^{x_0} h\,dx &= \frac{A}{2}. & \text{(2.35)}
\end{aligned}
$$

Then, as before,

$$\frac{h^3}{3\text{Ca}}\left(h_{xxx} - \text{Bo } h_x\right) = \text{const.} = 0,$$

The constant must be zero as the drop is of finite extent and thus $h = 0$ at some point (and all derivatives are assumed finite). Hence

$$h_{xxx} - \text{Bo } h_x = 0,$$

so that

$$h = a + b\sinh(x/\ell_c) + c\cosh(x/\ell_c),$$

where $\ell_c = \sqrt{1/\text{Bo}}$ is the dimensionless capillary length, as before. Equation (2.32) gives $b = 0$.

Then (2.33) and (2.34) give

$$a + c\cosh(x_0/\ell_c) = 0, \qquad \frac{c\sinh(x_0/\ell_c)}{\ell_c} = -\theta,$$

so that

$$c = -\frac{\theta\ell_c}{\sinh(x_0/\ell_c)}, \qquad a = \theta\ell_c\coth(x_0/\ell_c).$$

Finally x_0 is related to the cross sectional area A by

$$\begin{aligned} \frac{A}{2} &= \int_0^{x_0} [a + c\cosh(x/\ell_c)] \ \mathrm{d}x = ax_0 + c\ell_c\sinh(x_0/\ell_c) \\ &= \theta\ell_c^2\left[\frac{x_0}{\ell_c}\coth(x_0/\ell_c) - 1\right]. \end{aligned}$$

As $(y\coth(y) - 1)$ is monotonic increasing and attains all positive values for $y \geq 0$, we have that for any mass of fluid M there is a unique value x_0, which gives the width of the drop.

Static Axisymmetric Radial Drop, Bo $\ll 1$.

For later reference, consider an axisymmetric, static, radial drop of height $z = h(r)$, where r, θ, z are cylindrical polar coordinates. We also take Bo $\ll 1$ and assume the drop is sufficiently shallow to ensure the lubrication approximation holds. After non-dimensionalisation, we have

$$-p = \kappa \approx \nabla^2 h$$

and hence, by direct analogy to the previous calculations, the radial velocity and average radial velocity are given by

$$u = -\frac{z(z - 2h)}{2\text{Ca}}\frac{\partial}{\partial r}(\nabla^2 h), \qquad \bar{u} = -\frac{h^2}{3\text{Ca}}\frac{\partial}{\partial r}(\nabla^2 h).$$

As previously, use of the conservation equation and noting $\partial h/\partial t = 0$, as the drop is static, gives

$$0 = h^3\frac{\partial}{\partial r}(\nabla^2 h) = h^3\left[h_{rrr} - \frac{1}{r^2}h_r + \frac{1}{r}h_{rr}\right].$$

It is easily confirmed this is solved by

$$h = A(r_0^2 - r^2), \tag{2.36}$$

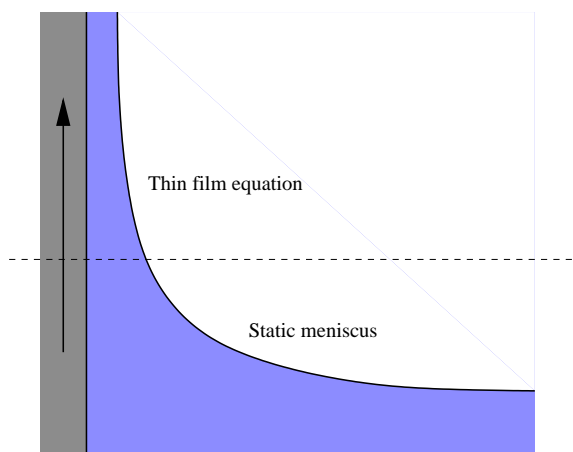which gives the shape of the drop, where the constants A, r_0 are constrained by the total drop volume.

Figure 2.8: Dip coating

2.3   The Landau–Levich equation

Consider now drawing a sheet at a constant speed out of a bath of fluid. This is a simple model of typical industrial coating processes. The main quantity of interest is the final thickness of the fluid film as a function of the withdrawal speed U.

We could redo our thin film analysis replacing the zero velocity no slip boundary condition with the condition $u = U$ on $z = 0$. However, we can avoid this by observing that in coordinates moving with the wall our previous equation holds. We proceed as follows:

1. We take equation (2.30) and impose $\alpha = \pi/2$ and $x \to -x$ to give

$$h_t + \left[\frac{h^3}{3\text{Ca}} \left(h_{xxx} - \text{Bo} \right) \right]_x = 0.$$

2. We use the plate velocity U as the non-dimensionalization velocity scale so that the plate velocity is unity in the non-dimensional equations. We jump to the travelling coordinate system

$$\bar{x} = x - t, \quad \bar{t} = t, \quad \bar{h}(\bar{x}, \bar{t}) = h(x, t).$$

In this frame we have zero velocity conditions on the plate $z = 0$ while the free surface conditions are unaffected, as we are still working in an inertial frame (and thus the force balances dictating the surface boundary conditions are the same). Hence, we can apply the above equation in this travelling coordinate system to find that

$$\bar{h}_{\bar{t}} + \left[\frac{\bar{h}^3}{3\text{Ca}} \left(\bar{h}_{\bar{x}\bar{x}\bar{x}} - \text{Bo} \right) \right]_{\bar{x}} = 0.$$

Transforming back to the laboratory frame we have that

$$h_t + h_x + \left[\frac{h^3}{3\text{Ca}} \left(h_{xxx} - \text{Bo} \right) \right]_x = 0$$

3. Following convention that horizontal directions are represented by x and vertical directions by z, we change the coordinate system $(x, z) \to (z, x)$ and thus we have

$$h_t + h_z + \left[\frac{h^3}{3\text{Ca}} \left(h_{zzz} - \text{Bo} \right) \right]_z = 0$$

as the final equation.

2.3.1   The steady state problem

Now suppose that the drag out settles down to a steady state. Then

$$h_z + \left[\frac{h^3}{3\text{Ca}} \left(h_{zzz} - \text{Bo} \right) \right]_z = 0. \tag{2.37}$$

An obvious scaling for the thickness of the fluid film is obtained by balancing gravity and viscosity, corresponding to choosing the scales so that $\text{Bo}/\text{Ca} = O(1)$. This gives

$$\frac{\rho g H^2}{\mu U} \sim 1,$$

so that

$$H \sim \left(\frac{\mu U}{\rho g} \right)^{1/2} = d,$$

say.

However, we will see that this is not the correct scaling in the case that the capillary number $\text{Ca} \ll 1$. We will develop a solution through the method of matched asymptotic expansions for the case $\text{Ca} \ll 1$. This solution will contain two regions: a thin film on the wall in which viscosity balances surface tension, and a static meniscus region in which surface tension balances gravity (see Figure 2.8).

2.3.2   The steady state drag out problem for $\text{Ca} \ll 1$.

Static meniscus, $\text{Ca} \ll 1$.

When $\text{Ca} \ll 1$, the fluid will adopt the shape of a static meniscus in which gravity and surface tension balance on the outer scale away from the wall. In particular the free surface condition shows that the velocity field does not contribute to the leading order dynamics and thus we have a hydrostatic problem at leading order.

We therefore use the Laplace–Young equation to describe the shape of the outer meniscus. (Note that we cannot use the general thin film equation here because our assumption of small slopes is violated in this capillary static region.) On taking our non-dimensionalization into account, the Laplace–Young equation (2.4) takes the form

$$\kappa = \text{Bo} f,$$
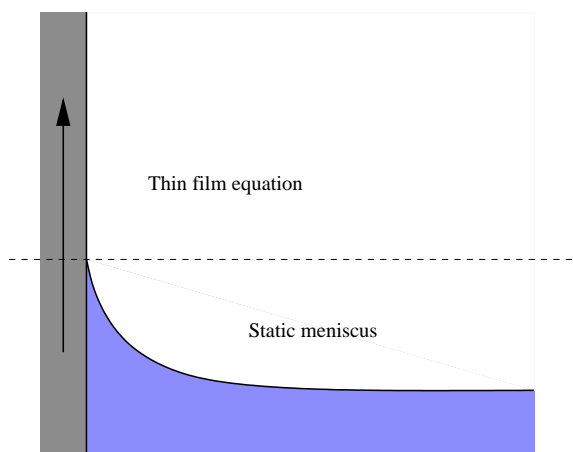
Figure 2.9: Meniscus region

where $z = f(x)$ is the height of the film. For the free surface to match with the thin film region the meniscus, as given by this equation, must be tangential at the point of contact.

Choosing the non-dimensionalization length scale R to enforce Bo $= 1$ (which is equivalent to choosing R to be the capillary length) gives $\kappa = f$. Instead of writing the height of the film as $z = f(x)$, let us write it as $x = H(z)$. Then the Laplace-Young equation is

$$\kappa = z,$$

or,

$$\frac{H_{zz}}{(1 + H_z^2)^{3/2}} = z \tag{2.38}$$

noting that the interpretation of curvature as the inverse radius of the best fit circle applies equally to a surface expressed in the form $z = f(x)$ or in the form $x = H(z)$. See Fig. 2.9. The boundary conditions for equation (2.38) are

$$H(z_0) \;\; = \;\; 0, \tag{2.39}$$

$$H'(z_0) \;\; = \;\; 0, \tag{2.40}$$

$$H \to \infty, \quad H_z \to -\infty \qquad \text{as } z \to 0, \tag{2.41}$$

where z_0 is the height of the (apparent) contact point above the free surface.

Integrating once gives

$$\frac{H_z}{(1 + H_z^2)^{1/2}} = \frac{z^2}{2} + A = \frac{z^2 - z_0^2}{2},$$

after using (2.40). Rearranging gives

$$H_z = \frac{z^2 - z_0^2}{\left[4 - (z_0^2 - z^2)^2\right]^{1/2}}.$$

As $z \to 0$ we find

$$H_z \sim -\frac{z_0^2}{(4 - z_0^4)^{1/2}}.$$

Applying (2.41) we see that we must choose $z_0 = \sqrt{2}$. This is now enough for us to determine the local behaviour near $z = z_0$, which is what we need for matching with (as yet undetermined) behaviour in the thin film region. Equation (2.38) gives

$$H_{zz}(z_0) = z_0 = \sqrt{2}.$$

Using the fact we now know $H(z_0)$, $H_z(z_0)$, $H_{zz}(z_0)$, we have

$$H \sim \frac{(z - z_0)^2}{\sqrt{2}}, \tag{2.42}$$

as $z \to z_0$.

Scaling of the wall region, Ca $\ll 1$.

As $z \to z_0$ the fluid forms a thin film on the wall. Let us determine the scaling of the thickness of this film, and the vertical extent of the "turn around" region where the thin film equation holds.

Rewriting (2.37) after recalling that Bo $= 1$ by our choice of non-dimensionalisation lengthscale, we have

$$h_z + \left(\frac{h^3}{3\mathrm{Ca}}\left(h_{zzz} - 1\right)\right)_z = 0. \tag{2.43}$$

We are interested in the behaviour as we approach the point z_0 and so we pose a rescaling of vertical length near z_0 by setting $z = z_0 + \epsilon \bar{z}$. (For the moment ϵ is not determined but we shall see that there is a natural choice.) Then, by (2.42),

$$h \sim \epsilon^2 \bar{z}^2$$

and we thus we set $h = \epsilon^2 \bar{h}$. On substituting these expressions into (2.43) we find that

$$\bar{h}_{\bar{z}} + \left[\frac{\epsilon^3 \bar{h}^3}{3\mathrm{Ca}}\left(\bar{h}_{\bar{z}\bar{z}\bar{z}} - \epsilon\right)\right]_{\bar{z}} = 0.$$

We can now determine the value of ϵ for a sensible balance of terms. For Ca $\ll 1$, surface tension is important in the dynamics, so we take

$$\epsilon = \mathrm{Ca}^{1/3} \ll 1.$$

This gives the thin film equation

$$\bar{h}_{\bar{z}} + \left[\frac{\bar{h}^3}{3} \left(\bar{h}_{\bar{z}\bar{z}\bar{z}} - \epsilon \right) \right]_{\bar{z}} = 0, \tag{2.44}$$

demonstrating that gravity is unimportant in the thin film region at leading order.

Solution in the wall region, Ca ≪ 1.

At leading order in (2.44) we have

$$\bar{h}_{\bar{z}} + \left(\frac{\bar{h}^3}{3} \bar{h}_{\bar{z}\bar{z}\bar{z}} \right)_{\bar{z}} = 0. \tag{2.45}$$

The solution of (2.45) needs to match with the meniscus region (2.42) as well as to a constant (undetermined) film thickness far up the wall. We therefore have the boundary conditions

$$\bar{h} \;\; \to \;\; \bar{h}_0 \text{ as } \bar{z} \to \infty, \tag{2.46}$$

$$\bar{h} \;\; \sim \;\; \frac{\bar{z}^2}{\sqrt{2}} \text{ as } \bar{z} \to -\infty, \tag{2.47}$$

where $\bar{h}_0$ is to be determined. Integrating (2.45) once gives

$$\bar{h} + \frac{\bar{h}^3}{3} \bar{h}_{\bar{z}\bar{z}\bar{z}} = \bar{h}_0, \tag{2.48}$$

by the condition at infinity. To examine the behaviour as $\bar{z} \to +\infty$, we linearize by setting $\bar{h} = \bar{h}_0 + f$ with $f \ll 1$. We find

$$f + \frac{\bar{h}_0^3}{3} f_{\bar{z}\bar{z}\bar{z}} = 0,$$

which has solution

$$f = a_* \exp\left[-3^{1/3} \bar{z}/\bar{h}_0 \right] + b_* \exp\left[3^{1/3} e^{i\pi/3} \bar{z}/\bar{h}_0 \right] + c_* \exp\left[3^{1/3} e^{-i\pi/3} \bar{z}/\bar{h}_0 \right].$$

Since the real part of the exponent is positive in the exponentials multiplying b_* and c_*, we must have $b_* = c_* = 0$ in order to satisfy the boundary condition at infinity.

End lecture 3

As $\bar{z} \to -\infty$, we linearise (2.48) by setting $\bar{h} = \bar{z}^2/\sqrt{2} + f$ with $|f| \ll \bar{z}^2$ and find

$$f_{\bar{z}\bar{z}\bar{z}} \sim \left[-\frac{6}{\bar{z}^4} - \frac{6\sqrt{2}h_0}{\bar{z}^6} \right] \sim -\frac{6}{\bar{z}^4},$$

with solution

$$f \sim a\bar{z}^2 + b\bar{z} + c + \frac{1}{\bar{z}},$$
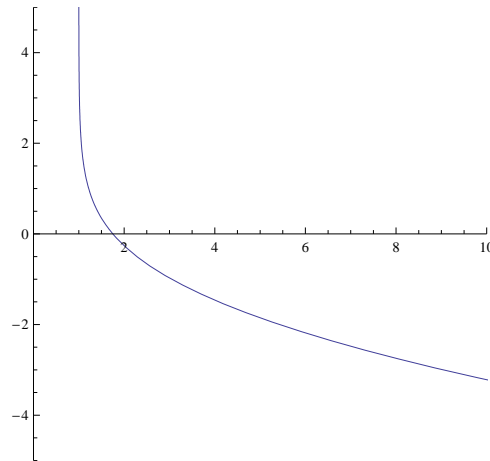
Figure 2.10: The solution close to the wall.

Since $|f| \ll \bar{z}^2$ we must have $a = 0$, but b and c are arbitrary.

Finally, equation (2.45) is translation invariant. Fixing the origin removes a degree of freedom; in fact, this is equivalent to fixing the coefficient a_* (as explicitly illustrated below).

Thus with the origin fixed, the boundary conditions contain two degrees of freedom, b and c, in the above. A final degree of freedom is in the choice of $\bar{h}_0$ and we have a third order differential equation. Thus we would expect (2.45) with the boundary conditions (2.46), (2.47) to have a solution only for a specific choice of $\bar{h}_0$, and this indeed turns out to be the case.

If we rescale (2.48) by writing $\bar{h} = \bar{h}_0 g$, $\bar{z} = \bar{h}_0 \zeta$ then we are seeking a solution to

$$g + \frac{g^3}{3} g''' \;\; = \;\; 1, \tag{2.49}$$

$$g \;\; \sim \;\; 1 + e^{-3^{1/3}\zeta} \qquad \text{as } \zeta \to \infty, \tag{2.50}$$

$$g \;\; \sim \;\; \frac{\bar{h}_0}{\sqrt{2}} \zeta^2 \qquad \text{as } \zeta \to -\infty, \tag{2.51}$$

where we have set the coefficient a_* to unity by utilising the translational freedom to change the origin.

Note that solutions of (2.49) with $g \to \infty$ will satisfy $g''' \to 0$, i.e. $g \propto \zeta^2$. Numerically shooting from infinity we find that the solution to (2.49), subject to (2.50), satisfies

$$g \sim 0.67 \zeta^2 \qquad \text{as } \zeta \to -\infty.$$

Thus $\bar{h}_0 = 0.67\sqrt{2} \approx 0.948$ and $h_0 \approx 0.948\mathrm{Ca}^{2/3}$. Redimensionalising we see that the dimensional film thickness is

$$h_0 \ell_c = 0.948 \left(\frac{\mu U}{\gamma}\right)^{2/3} \left(\frac{\gamma}{\rho g}\right)^{1/2} = 0.948 \frac{\mu^{2/3} U^{2/3}}{\gamma^{1/6} \rho^{1/2} g^{1/2}}.$$

We note that the dimensional height satisfies

$$0.948 \left(\frac{\mu U}{\gamma}\right)^{1/6} \left(\frac{\mu U}{\rho g}\right)^{1/2} \sim \mathrm{Ca}^{1/6} d,$$

so that the film is much thinner in the limit $\mathrm{Ca} \to 0$ than the thickness d, which we obtained initial by naively balancing viscosity and gravity in §2.3.1.

2.4   Moving contact lines

2.4.1   The problem

We saw in Section 2.2.4 that a drop of fluid will sit in equilibrium on a substrate with the final shape depending on the contact angle.

We would like to be able to model the evolution of such a configuration, that is, given an initial finite drop of fluid, can we model it as it spreads to find this final shape.

One might think that we could do this by simply applying the boundary conditions

$$h = 0, \qquad h_x = \Theta,$$

at the unknown boundary of the fluid drop (as well as requiring that there is no mass loss at the interface). However, such boundary conditions are not compatible with equation (2.31): they do not allow the contact line to move, as we will now show.

   Let us suppose that the boundary of the fluid is located at $x = s(t)$. Then, if we zoom in on the interface by setting $x = s(t) + \xi$ with ξ small then locally $h \sim \Theta\xi$. Setting $h = \Theta\xi + f$, with $\xi \ll 1$, $|f| \ll \Theta\xi$ and keeping only the leading and next to leading terms gives

$$f_t - \dot{s}f_\xi - \dot{s}\Theta + \left[\frac{\Theta^3 \xi^3}{3\mathrm{Ca}} f_{\xi\xi\xi} - \frac{\Theta^3}{3\mathrm{Ca}}\mathrm{Bo}(\xi^3 f)_\xi\right]_\xi - \frac{\mathrm{Bo}}{\mathrm{Ca}}\Theta^4 \xi^2 = O(f^2).$$

For $\xi \ll 1$, $f \ll \Theta\xi$, this simplifies to give

$$f_t - \dot{s}f_\xi + \left[\frac{\Theta^3 \xi^3}{3\mathrm{Ca}} f_{\xi\xi\xi}\right]_\xi = \dot{s}\Theta.$$

Attempting to neglect the higher spatial derivatives gives the hyperbolic equation $f_t - \dot{s}f_\xi = \dot{s}\Theta$, with $f = 0$ at $\xi = 0$, which has solution $f = -\Theta\xi$; this is incompatible with $|f| \ll \Theta\xi$, as is

$$f_t - \dot{s}f_\xi \approx \dot{s}\Theta.$$

Hence, we must have that the higher spatial derivative term and $\dot{s}\Theta$ are of the same order:

$$\left(\frac{\Theta^3\xi^3}{3\mathrm{Ca}}f_{\xi\xi\xi}\right)_\xi \sim \dot{s}\Theta,$$

and thus

$$f_{\xi\xi\xi} \sim \frac{3\mathrm{Ca}\,\dot{s}}{\Theta^2\xi^2}.$$

i.e.

$$f \sim \frac{3\mathrm{Ca}\,\dot{s}}{\Theta^2}\left(\xi\log\xi - \xi\right) \sim \frac{3\mathrm{Ca}\,\dot{s}}{\Theta^2}\xi\log\xi. \tag{2.52}$$

However, f is supposed to be much smaller than h, and $h \sim \Theta\xi \ggg O(\xi\log\xi)$. We conclude that balancing surface tension on the left with the dominant term on the right is inconsistent.

Supposing that it is the gravity term on the left of the above equation that balances the dominant term on the right we have that

$$f_\xi \sim -\frac{3\mathrm{Ca}\,\dot{s}}{\mathrm{Bo}\Theta^2\xi^2},$$

which is even more singular.

Having both terms on the left at a higher order of magnitude with significant cancellation is even more singular. Hence, we have that we cannot find a consistent solution local to the moving contact line.

The difficulty does not lie in our attempt to use thin film theory or even inadequate mathematics; it is a fundamental physical difficulty. The non-slip boundary condition on the one hand, and the free surface boundary condition on the other, involve very different physics. It is perhaps no surprise that very near a moving contact line, where the influences of both the solid-fluid interface and the free surface interface are both present, the fundamental physics underlying the Navier-Stokes boundary conditions needs to be captured; fortunately, it nonetheless appears that continuum mechanics is still valid in this region. We will only look at very special cases of the additional physics considered in attempts to resolve this cutting edge problem; (see Ralston et. al. Annu. Rev. Mater. Res. 2008. for a comprehensive review).

2.4.2   Precursor film

A simple way of introducing the additional physics required for a well defined model of a moving contact line is to postulate that the unwetted portion of the boundary actually has a very thin layer of fluid covering it. For instance during the oscillatory motion of a moving contact line, it is reasonable to hypothesis a thin film remains covering the substrate; providing it is legitimate to treat the thin film in the context of continuum mechanics then the fluid dynamical equations can be solved everywhere, and the problem of a contact line has been removed.

2.4.3   Slip

Another hypothesis for the physics required to treat the moving contact line is to allow a small amount of slip between the substrate and the fluid. Rather than imposing $u = 0$ on $z = 0$ a slip law relating horizontal velocity to the shear stress is postulated, such as

$$u = \lambda u_z. \tag{2.53}$$

Using this law the thin film equation becomes (see exercises)

$$h_t + \left[\frac{1}{\mathrm{Ca}} \left(\frac{h^3}{3} + \lambda h^2 \right) (h_{xxx} - \mathrm{Bo}h_x) \right]_x = 0. \tag{2.54}$$

Now, on expanding locally, there is a dominant balance

$$\lambda \Theta^2 \xi^2 f_{\xi\xi\xi} \sim \mathrm{Ca}\, \dot{s}\Theta\xi,$$

so that

$$f_{\xi\xi} \sim \frac{\mathrm{Ca}\, \dot{s}}{\Theta\lambda} \log \xi,$$

$$f \sim \frac{\mathrm{Ca}\, \dot{s}}{\Theta\lambda} \xi^2 \log \xi \ll \Theta\xi,$$

for small ξ, and it is possible to impose a contact angle Θ. However, for small values of λ, there is a boundary layer near the contact line, and the local value of the contact angle is not the same as the one that the outer solution sees.

End lecture 4

2.4.4   Tanner's law

Often, in addition to a regularisation such as slip, a fixed contact angle is not imposed but a relationship between the velocity of the contact line and the contact angle is postulated.

Tanner's law[1] is one such commonly used relationship between the contact angle and the velocity of the boundary and has often been observed to hold in specific contexts. It states

$$v = K \left(\theta^3 - \Theta^3 \right),$$

where v is the normal velocity of the boundary, θ is the actual contact angle, and Θ is the static contact angle. In the thin film approximation this becomes

$$v = K \left(-h_x^3 - \Theta^3 \right).$$

Tanner's law gives a natural velocity scale

$$U = K.$$

---

[1]Sometimes also referred to as the Cox–Voinov law, see, for example, Snoeijer and Andreotti, *Annu. Rev. Fluid Mech.* **45**, 269 (2013).

Using this scale in the nondimensionalisation of the thin film equation, the nondimensional version of Tanner's law is simply

$$v = -h_x^3 - \Theta^3,$$

and the motion will be quasistatic if

$$\mathrm{Ca} = \frac{\mu U}{\gamma} = \frac{\mu K}{\gamma} \ll 1.$$

Again the large influence of surface tension dominates the equations giving a hydrostatic balance at leading orders.

2.4.5   Quasistatic evolution with $\mathrm{Ca} \ll 1$, $\mathrm{Bo} \ll 1$

Even when using Tanner's law in the full time dependent problem it is still necessary to allow some slip to avoid a contact line singularity. However, we have seen that the law of motion of the contact line will contain a natural velocity scale, and if this is slower than the scale obtained by balancing viscosity with surface tension (i.e. the scale obtained by setting $\mathrm{Ca} = 1$) then the fluid may move quasi-statically: for a given contact line we solve the steady version of (2.31), which will have a certain contact angle. The contact line then moves with a speed determined by this contact angle. In the quasi-static case there is no problem with stress singularities, and we do not need to include slip.

Thus, for symmetric quasi-static drop spreading using Tanner's law and the lengthscale chosen so that $\mathrm{Bo} \ll 1$ we need to solve

$$\left[\frac{h^3}{3\mathrm{Ca}} h_{xxx} \right]_x = 0, \tag{2.55}$$

with

$$
\begin{aligned}
h(s) &= 0, \\
\dot{s} &= -h_x^3 - \Theta^3,
\end{aligned}
\tag{2.56}
$$

at the contact line $x = s(t)$, together with a global mass balance equation

$$\int_{-s}^{s} h \, \mathrm{d}x = A.$$

We find that

$$h = \frac{\theta}{2s}(s^2 - x^2),$$

where $\theta = -h_x(s)$.

(Note that the choice of $\mathrm{Bo} \ll 1$ corresponds to a drop that is small compared to the capillary length ℓ_c. The above result can be reconciled with the result derived in §2.2.4 by considering the $s(t) \ll \ell_c$ limit of the results discussed there.)
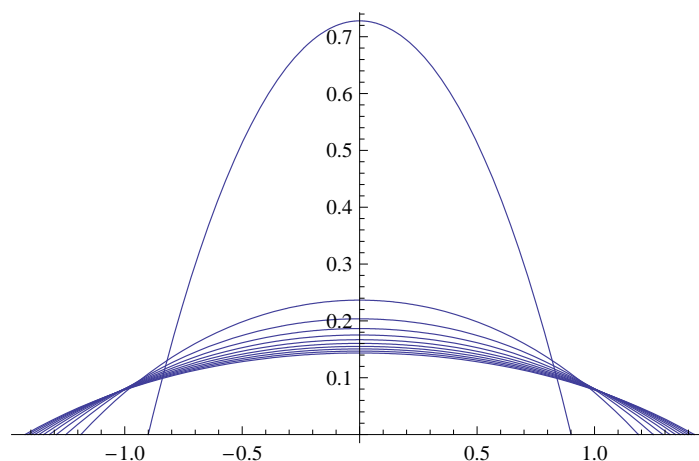
Figure 2.11: Drop spreading

Imposing the total mass constraint gives

$$A = \frac{2}{3}\theta s^2 \tag{2.57}$$

Tanner's law (2.56) then gives the evolution equation for s as

$$\dot{s} = \theta^3 - \Theta^3 = \frac{27 A^3}{8 s^6} - \Theta^3. \tag{2.58}$$

This represents an ordinary differential equation for the evolution of the contact line position $s(t)$ given an initial condition $s(0) = s_0$. Clearly there is an equilibrium value of s, s_∞, for which $\dot{s} = 0$.

2.4.6 Evaporating drops and coffee stains. Ca $\ll$ 1, Bo $\ll$ 1.

Why is it that when split coffee dries the stain always has a dark rim? In this section we will try and answer this question.

Suppose (not unreasonably) that we have a drop which is slowly evaporating, so that the motion is quasi-static. If the evaporation is slow by comparison to the motion of the contact line, then the drop will move through a sequence of steady state profiles, given by the steady state version of (2.31) as in Section 2.2.4.

Now though, because of evaporation, the mass of fluid is not constant but decreasing. Suppose that the rate of evaporation is uniform across the surface of the drop (in practice there will be more evaporation from the edges that from the centre). Then the mass balance equation becomes

$$\frac{\mathrm{d}}{\mathrm{d}t} \int_{-s}^{s} h \ \mathrm{d}x = -\int_{-s}^{s} E \left(1 + h_x^2\right)^{1/2} \ \mathrm{d}x \approx -\int_{-s}^{s} E \ \mathrm{d}x = -2sE,$$

where E is the evaporation rate and the thin film approximation $h_x \ll 1$ has been invoked. Since the motion is quasi-static, E determines the timescale for the evolution of the drop; using a velocity scaling based on E we can therefore set $E = 1$ in the non-dimensional equations, which we do henceforth.

For the sake of simplicity let us assume that Bo $\ll 1$, so that gravity is negligible. The steady solution for a drop of length $2s$ then emerges from the equation $(h^3 h_{xxx}/3\text{Ca})_x = 0$; integrating and noting that $h = 0$ at $x = \pm s$ to set the constant of integration equal to zero, one has $h_{xxx} = 0$. For simplicity, we shall also assume that the contact angle $\theta = \Theta$, the equilibrium value and hence is constant: the dynamics is driven solely by evaporation. Using symmetry and the boundary conditions at $\pm s$, including setting the contact angle $h_x = \pm\Theta$ at $x = \mp s$ gives

$$h = \frac{\Theta}{2s}(s^2 - x^2). \tag{2.59}$$

Thus, if we allow s to vary slowly, the mass loss is

$$-2s = \frac{\mathrm{d}}{\mathrm{d}t} \int_{-s}^{s} h \ \mathrm{d}x = \frac{\mathrm{d}}{\mathrm{d}t} \left[\frac{\Theta}{2s} \left(s^2 x - \frac{x^3}{3} \right) \right]_{-s}^{s} = \frac{\mathrm{d}}{\mathrm{d}t} \left(\frac{2\Theta s^2}{3} \right) = \frac{4\Theta s \dot{s}}{3},$$

so that

$$\dot{s} = -\frac{3}{2\Theta},$$

and the length of the drop shrinks linearly to zero.

Let us examine the flow of liquid during this shrinking. The full evolution equation for the flow (incorporating a sink due to evaporation) is

$$h_t + (h\bar{u})_x = h_t + \left(\frac{1}{3\text{Ca}} h^3 h_{xxx} \right)_x = -1.$$

Expanding

$$h \sim h_0 + \text{Ca} \ h_1 + \cdots, \qquad q = \frac{1}{3} h^2 h_{xxx} \sim q_0 + \text{Ca} \ q_1 + \cdots,$$

we have the quasi-static solution at leading order

$$h_0 q_0 = \frac{h_0^3}{3} h_{0,xxx} = 0,$$

which leads to the solution (2.59). At first order we find

$$h_{0,t} + (h_0 q_1)_x = -1,$$

since the $h_1 q_0$ term disappears. The flow field is given by $\bar{u} \sim q_0/\text{Ca} + q_1 \sim q_1$ without a need to determine the correction to the height h_1. Using the leading order profile in (2.59) we have

$$(h_0 q_1)_x = -1 - h_{0,t} = -1 - \frac{\Theta}{2} \dot{s} - \frac{\Theta}{2} \frac{x^2}{s^2} \dot{s}$$

Figure 2.12: Evaporation of a film with a fixed contact angle. Since mass is lost uniformly from the surface, but there is more mass difference between the profiles near the contact line, fluid must flow from the edge to the centre.

Recalling that

$$\dot{s} = -\frac{3}{2\Theta}$$

we have

$$\bar{u} \sim q_1 = \frac{2s}{\Theta(s^2 - x^2)} \int_0^x \left(-1 - \frac{\Theta}{2}\dot{s} - \frac{\Theta}{2}\frac{\bar{x}^2}{s^2}\dot{s} \right) d\bar{x}$$

$$= -\frac{2sx}{\Theta(s^2 - x^2)} \left(\frac{1}{4} - \frac{x^2}{4s^2} \right)$$

$$= -\frac{x}{2s\Theta},$$

where we have used the fact that, by symmetry, $\bar{u}(0) = 0$. This means that the flow is inwards from the contact line to the centre; we should expect that a dark spot in the middle of a coffee stain. This is the opposite of what is observed in 'experiments'. How do we resolve this discrepancy?

Advancing and receding contact angles

It is often observed that the advancing contact angle is different from the receding contact angle, so that the motion of the contact line might be described by

$$v = \begin{cases} -K_R(\theta_R^3 - \theta^3), & \theta < \theta_R, \\ 0, & \theta_R < \theta < \theta_A, \\ K_A(\theta^3 - \theta_A^3), & \theta_A < \theta. \end{cases} \tag{2.60}$$
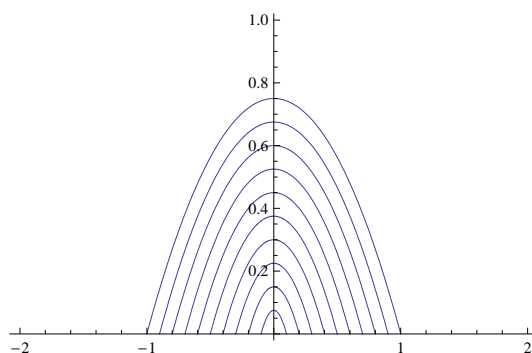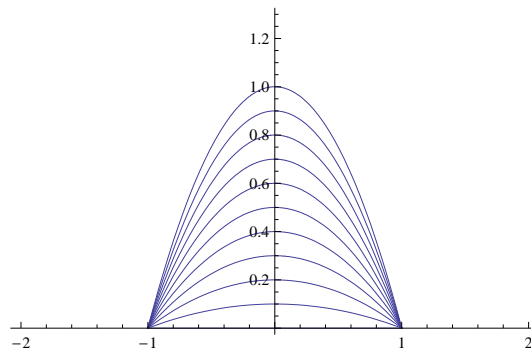
Figure 2.13: Evaporation of a film with a pinned contact line. Since mass is lost uniformly from the surface, but there is less mass difference between the profiles near the contact line, fluid must flow from the centre to the edge.

This is what is happening in the coffee case. When the stain evaporates the contact angle first changes gradually from the advancing to the receding contact angle before the contact line finally recedes. Thus there is a significant time during which the contact line is pinned.

We can redo the analysis of the previous section with a given contact length, with a pinned contact line and varying contact angle (see Problem Sheet 3). Now the quasi-steady solution is of the form

$$h = \frac{3A(t)}{4s^3}(s^2 - x^2),$$

where s is independent of time. Note that since the position of the contact line is fixed, the contact angle θ must change as $A(t)$ changes. This does not give a contradiction provided that the resulting value of $\theta = -3A(t)/2s^2$ lies in the the range of contact angles for which the contact line is pinned, see (2.60).

Then, with a use of the thin film approximation and a velocity scaling such that the dimensionless evaporation rate is unity, mass conservation gives

$$-2s = \frac{\mathrm{d}}{\mathrm{d}t} \int_{-s}^{s} h \ \mathrm{d}x = \dot{A}.$$

One can show that the mean velocity is now given by

$$\bar{u}_1 = \frac{2sx}{3A}$$

and the flow is outward towards the contact line, carrying dissolved coffee to the rim of the drop where it is deposited as the liquid evaporates. This *is* what is observed experimentally.

A more detailed model of this problem (incorporating non-uniform evaporation rates) was presented by R. D. Deegan *et al.*, *Nature* **389**, 827 (1998).

3 Flow in Porous Media

3.1 The basics: Darcy's law

The flow within a porous medium may be modelled by Darcy's law

$$\mathbf{u} = -\frac{k}{\mu}\left(\nabla p + \rho g \boldsymbol{e}_z\right) \tag{3.1}$$

for some constant k (called the *permeability*). This will be deduced below for low Reynolds number and constant density and is to be solved along with the incompressibility of the liquid, i.e.

$$0 = \nabla \cdot \mathbf{u} = -\frac{k}{\mu}\nabla^2 p$$

and with the boundary condition that the normal liquid velocity should be continuous at rigid boundaries, i.e.

$$[\mathbf{u} \cdot \mathbf{n}]_-^+ = 0,$$

or that the pressure, p, be given at free surfaces.

It is useful to note that when the density of the liquid in question does not vary spatially then we may rewrite (3.1) as

$$\mathbf{u} = -\frac{k}{\mu}\nabla(p + \rho g z). \tag{3.2}$$

To a certain extent, (3.1) is a phenomenological law that satisfies two basic requirements:

(i) flows are driven by pressure gradients (from high pressure to low) and

(ii) the flow speed for a given pressure gradient decreases with increasing liquid viscosity μ.

For small Reynolds number flows this law is found to be in good agreement with experimental data. Here, however, we shall present a plausible derivation of Darcy's law for constant density and low Reynolds number based on the technique of homogenization — averaging the behaviour at the micro-scale to obtain a law applicable at the macro-scale.

3.1.1 Homogenization

We begin from the Navier–Stokes equations for an incompressible Newtonian fluid of constant density ρ sitting within a rigid porous medium. We have that

$$\rho \mathbf{u}_t + \rho \mathbf{u} \cdot \nabla \mathbf{u} = -\nabla[p + \rho g z] + \mu \nabla^2 \mathbf{u}, \quad \nabla \cdot \mathbf{u} = 0, \tag{3.3}$$

and we let

$$p^* = p + \rho g z$$

below. Equation (3.3) must be solved subject to the no-slip boundary condition on the surface, S, of the porous medium, i.e.

$$\mathbf{u} = 0, \quad \mathbf{x} \in S. \tag{3.4}$$

Qualitatively, we expect that the pressure gradient will be imposed on a relatively long length scale, L, while the dominant length scale for viscous dissipation in (3.3) is the size of the pores r_p, where we require that $\epsilon = r_p/L \ll 1$. We expect that the pores are small, in which case the pore scale flow will be governed by Stokes equations (i.e. inertia is negligible). Scaling (3.3) for low Re flow gives an estimate for the typical flow speed, U, induced by a pressure scale for p^*, denoted P. This is therefore given by

$$\frac{P}{L} \sim \frac{\mu U}{r_p^2} \implies U \sim \frac{r_p^2 P}{\mu L}.$$

We use the scales P, U and r_p to non-dimensionalize the momentum equation in (3.3), together with the timescale r_p/U, to deduce

$$\mathrm{Re}\,(\mathbf{u}_t + \mathbf{u}{\cdot}\nabla\mathbf{u}) = -\epsilon^{-1}\nabla p^* + \nabla^2\mathbf{u} \tag{3.5}$$

where

$$\mathrm{Re} = \frac{\rho U r_p}{\mu} = \epsilon\frac{\rho r_p^2 P}{\mu^2}$$

is the pore scale Reynolds number (i.e. the Reynolds number based on the pore length scale r_p, rather than the macroscopic length scale L). In what follows, we shall assume that $\mathrm{Re} \leq O(\epsilon)$ so that the inertial terms in (3.5) can be neglected.

To make progress we shall assume that

- the porous matrix and the flow is periodic on the pore lengthscale r_p,

- the periodic cell is a cuboidal box, V, with typical linear dimension $O(r_p)$.

- $\mathbf{u}$, p are periodic on the scale of a few cells, although again they may vary on the longer scale L.

- $\mathrm{Re} \sim O(\epsilon)$.

In addition we will, in principle, allow the structure to change on the macroscopic length scale L. To capture the two different length scales, r_p, L, we shall introduce the variables

$$\mathbf{x}, \quad \mathbf{X} = \epsilon\mathbf{x}$$

and allow all of our state variable (velocity, pressure, etc.) to be functions of *both* $\mathbf{x}$, the microscale variable, and $\mathbf{X}$, the macroscale variable. We then pose power series expansions for $\mathbf{u}$ and p^*:

$$\mathbf{u} = \mathbf{u}^0 + \epsilon\mathbf{u}^1 + \epsilon^2\mathbf{u}^2 + ...$$

and

$$p^* = p^{*0} + \epsilon p^{*1} + \epsilon^2 p^{*2} + \ldots$$

with the $\mathbf{u}^{(j)}$ and $p^{(j)}$ all being functions of both $\mathbf{x}$ and $\mathbf{X}$. At the two highest orders in ϵ, i.e. $O(\epsilon^{-1})$ and $O(\epsilon^0)$, the momentum equation (3.5) gives

$$\frac{\partial p^{*0}}{\partial \mathbf{x}} = 0, \quad \frac{\partial p^{*1}}{\partial \mathbf{x}} = -\frac{\partial p^{*0}}{\partial \mathbf{X}} + \nabla_{\mathbf{x}}^2 \mathbf{u}^0, \tag{3.6}$$

respectively. (Here we use the notation $\partial/\partial\mathbf{x}$ to denote the gradient with respect to the coordinate system $\mathbf{x}$.) Similarly, incompressibility gives

$$\nabla_{\mathbf{x}} \cdot \mathbf{u}^0 = 0, \quad \nabla_{\mathbf{x}} \cdot \mathbf{u}^{(1)} = -\nabla_{\mathbf{X}} \cdot \mathbf{u}^0. \tag{3.7}$$

We note that the equations (3.6) and (3.7) are only linear because of our assumption that $\mathrm{Re} \leq O(\epsilon)$. Nonlinear effects will enter at $O(\epsilon^2)$ in the present analysis — fortunately, we do not need to go this far.

Now, (3.6)a may be integrated once to show that

$$p^{*0} = p^{*0}(\mathbf{X}).$$

Eqn. (3.6)b is a linear Stokes flow equation, forced by the large scale pressure gradient

$$-\frac{\partial p^{*0}}{\partial \mathbf{X}},$$

which is also consistent with the underlying physics of pressure driven flow. By linearity, we can write $\mathbf{u}^0$ and p^{*1} as a matrix multiple of and dot product with $\partial p^{*0}/\partial\mathbf{X}$, respectively

$$u_i^0 = -K_{ij}(\mathbf{x}, \mathbf{X})\frac{\partial p^{*0}}{\partial X_j} + B_i(\mathbf{X}, \mathbf{x}), \qquad p^{*1} = -A_j(\mathbf{x}, \mathbf{X})\frac{\partial p^{*0}}{\partial X_j} + \bar{p}^{*1}(\mathbf{x}, \mathbf{X}). \tag{3.8}$$

where the additional terms $B_i(\mathbf{X}, \mathbf{x})$, $\bar{p}^{*1}(\mathbf{X}, \mathbf{x})$ are freedoms (sometimes refereed to as gauge freedoms) that are not fixed by Eqn. (3.6)b. However, since the flow is driven by the large scale pressure gradient, and thus is zero with it, $B_i(\mathbf{X}, \mathbf{x})$ will be zero providing this is consistent with all boundary conditions, which holds as we will see below. With $B_i(\mathbf{X}, \mathbf{x}) = 0$ we have $\bar{p}^{*1} = \bar{p}^{*1}(\mathbf{X})$ by Eqn. (3.6)b.

Thus we proceed with

$$u_i^0 = -K_{ij}(\mathbf{x}, \mathbf{X})\frac{\partial p^{*0}}{\partial X_j}, \qquad p^{*1} = -A_j(\mathbf{x}, \mathbf{X})\frac{\partial p^{*0}}{\partial X_j} + \bar{p}^{*1}(\mathbf{X}). \tag{3.9}$$

Substituting the solution form (3.9) into (3.6) and (3.7) we obtain equations for K_{ij} and A_j, which can in principle be solved for a given pore geometry (see, for example, Lee *et al.*, *Int. J. Heat Mass Transfer* **39**, 661 (1995)). However, for our purposes it is enough to stick to the form given in (3.9) and consider averages over the periodic cell volume V, which we take to be cuboid so that it tessellates with periodicity in each Cartesian axis.

We now introduce the average over a cell

$$\langle f \rangle = \frac{1}{|V|} \int_{V_f} f \, \mathrm{d}V \tag{3.10}$$

where V_f is the volume of fluid within the cell V. Since the functions p^{*0} and $\bar{p}^{*1}$ are functions of the large scale only (and *not* the pore scale) we immediately have that

$$\langle u_i^0 \rangle = -\langle K_{ij} \rangle \frac{\partial p^{*0}}{\partial X_j}, \quad \langle p^{*1} \rangle = -\langle A_j \rangle \frac{\partial p^{*0}}{\partial X_j} + \phi \bar{p}^{*1} \tag{3.11}$$

where $\phi = V_f/V$ is the *porosity* of the medium — the fraction of the unit cell that is filled by voids and hence by fluid. We note that (3.11) already has the form of Darcy's law. The final check that needs to be performed is the averaging of (3.7)b, which gives

$$\nabla \cdot \langle \mathbf{u}^0 \rangle = -\frac{1}{|V|} \int_{V_f} \nabla \cdot \mathbf{u}^1 \, \mathrm{d}V = -\frac{1}{|V|} \int_S \mathbf{u}^1 \cdot \mathbf{n} \, \mathrm{d}S = 0 \tag{3.12}$$

where we have used the Divergence theorem for the first equality. On boundaries of the cuboid cell, V_f, that is the cuboidal shell $S = \partial V_f$, that coincide with the solid matrix, $\mathbf{u} = \mathbf{0}$ as there is no normal or tangential flow, and thus no contribution to the integral. On all other regions of S flow periodicity on the pore scale entails that $\mathbf{u}, \mathbf{u}^0, \mathbf{u}^1, \ldots$ on the cuboidal shell S are equal to $\mathbf{u}, \mathbf{u}^0, \mathbf{u}^1, \ldots$ at the equivalent point on the opposite face of S, where the normal has switched sign, so that once more there is no contribution to the integral over S, which is thus zero.

In this course we shall only be concerned with homogeneous, isotropic media so that

$$\langle K_{ij}(\mathbf{x}, \mathbf{X}) \rangle = K \delta_{ij},$$

where K is a constant. In this case the leading order equation becomes a dimensionless version of Darcy's law

$$\mathbf{u} = -K \nabla p^*. \tag{3.13}$$

and we also have

$$0 = \nabla \cdot \mathbf{u},$$

where superscripts have been dropped (since we are only interested in the leading order behaviour) and averages (since we are only interested in the behaviour on the macroscopic scale). For completeness we rewrite (3.13) in dimensional terms:

$$\mathbf{u} = -\frac{k}{\mu} \nabla p^* = -\frac{k}{\mu} \nabla(p + \rho g z), \quad 0 = \nabla \cdot \mathbf{u} = -\frac{k}{\mu} \nabla^2 (p + \rho g z) = -\frac{k}{\mu} \nabla^2 p, \tag{3.14}$$

where the permeability $k = r_p^2 K$. We see immediately that the behaviour is determined entirely by the pressure and gravity and that Equation (3.14) is precisely the form of (3.1) for constant density. We also note that the permeability k scales with the square of the typical pore size, r_p — a relatively sensitive dependence, as is observed experimentally.

It is important to note that the velocity given by (3.14) is actually the average fluid velocity over the periodic cell volume V. This velocity is referred to as the *macroscale Darcy velocity* and is *not* equal to the average microscale fluid velocity within the pores, which is given by

$$\mathbf{u}_{Microscale} = \frac{1}{\phi} \mathbf{u}_{Macroscale\ Darcy} = \frac{1}{\phi} \mathbf{u}.$$

Intuitively, the average microscale fluid velocity must be larger than the macroscale Darcy velocity since it has to give the appearance of a fluid flux over a larger volume than it has available to it.

3.1.2 Example: Flow focusing

Consider a porous medium which has uniform, isotropic permeability k everywhere except within a cylindrical inclusion of radius a in which the permeability is k'. Imagine that far from the cylindrical inclusion a uniform flow $\mathbf{U} = U\boldsymbol{e}_x$ occurs. We would like to quantify the influence of the inclusion on the flow-field.

Since the problem is steady, there is no gravity and the velocity field is given by Darcy's law (3.1) subject to incompressibility $\nabla \cdot \mathbf{u} = 0$ we have that the pressure field p must satisfy Laplace's equation

$$\nabla^2 p = 0.$$

This problem is very familiar from the potential flow problems considered in Part A Fluid Dynamics & Waves: here the pressure p is playing the role of the velocity potential ϕ in that course. Indeed, since $\mathbf{u} = \nabla(-kp/\mu)$ the effective velocity potential is $\phi = -kp/\mu$.

Far from the cylindrical inclusion we require that $\phi = -kp/\mu \sim Ux$ while at the boundary of the inclusion we must have that the pressure and normal velocity are continuous, i.e.

$$[p]_{a^-}^{a^+} = 0, \quad [\mathbf{n}\cdot\nabla\phi]_{a^-}^{a^+} = 0 \implies \left.\frac{\partial\phi}{\partial r}\right|_{r=a^+} = \left.\frac{\partial\phi}{\partial r}\right|_{r=a^-}$$

The relevant solutions of Laplace's equation have the form

$$\phi = -kp/\mu = (Ar + B/r)\cos\theta$$

with the $\cos\theta$ term arising because of the condition at ∞. The coefficients A and B will depend on whether we are in the region $r > a$ or $r < a$. We therefore introduce $A_<, B_<$ and $A_>, B_>$ to be used when $r < a$ and $r > a$, respectively.

For $r > a$ we must have $A_> = U$ to match the condition at $r = \infty$ while for $r < a$ we must have $B_< = 0$ to avoid a divergence in the velocity field as $r \to 0$. We therefore have from the continuity of pressure boundary condition that

$$Ua + B_>/a = A_< a\frac{k}{k'}$$

while the continuity of normal velocity requires that

$$U - B_>/a^2 = A_<.$$

Solving these equations simultaneously, we find that

$$\phi = -kp/\mu = \begin{cases} U\frac{2k'}{k+k'}r\cos\theta, & r < a \\ U\left(r + \frac{k-k'}{k+k'}\frac{a^2}{r}\right)\cos\theta, & r > a. \end{cases} \tag{3.15}$$

Note that in the limit $k = k'$, i.e. the inclusion has the same permeability as the medium, the result reduces to $\phi = Ur\cos\theta$ everywhere as should be expected. If $k'/k \ll 1$, so that the inclusion is effectively impermeable, then we recover the classic result for potential flow past a rigid cylinder.
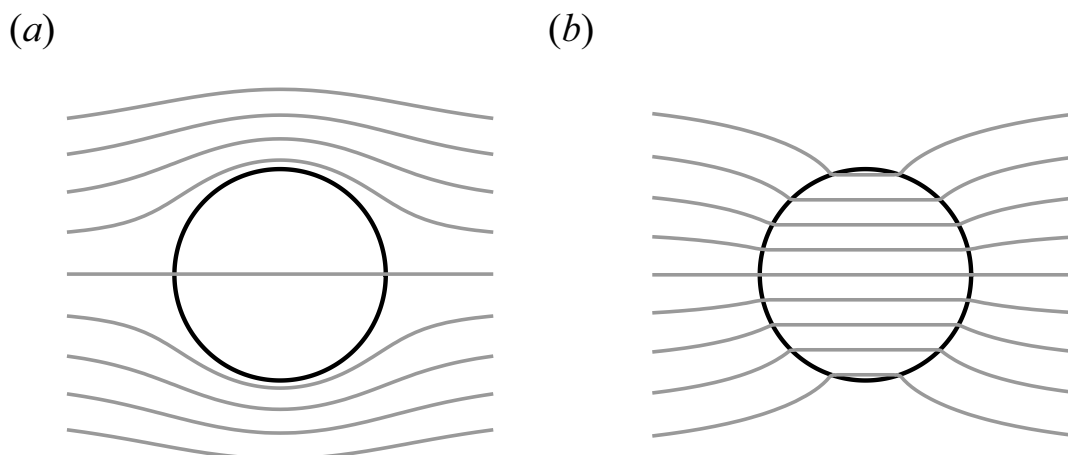
(*a*)   (*b*)

Figure 3.1: Streamlines for the effect on uniform flow in a porous medium (permeability k) of a cylindrical inclusion with permeability k'. (a) A relatively impermeable inclusion, $k'/k = 0.1$, diverts the flow. (b) A relatively permeable inclusion, $k'/k = 10$, demonstrates the phenomenon of flow focussing, which plays a role in a number of instabilities in porous media.

By plotting the streamlines of these flows in the cases $k > k'$ and $k < k'$ we see that the inclusion either 'focuses' the flow (if $k' > k$) or diverts it (if $k > k'$) — see figure 3.1. This is an important mechanism for instability within soluble porous media since if the medium is dissolved by, for example, acid, it becomes more permeable and hence more acid flows through that region dissolving yet more porous medium. This instability has been studied by numerous authors (see, for example, Hinch & Bhatt, *J. Fluid Mech.* **212**, 279, 1990). Flow focusing can also be useful because the Reynolds number increases locally, potentially facilitating the mixing of two components.

3.2 Thermal convection

Convection is a problem of interest in a wide range of applications from understanding the convection that happens within the Earth's mantle to how geothermal heating (or radioactive waste!) can drive flows within saturated rock.

For simplicity, we shall assume a linear relationship between the density ρ of the liquid and temperature T,

$$\rho = \rho_0 \left[1 - \beta(T - T_0) \right], \tag{3.16}$$

where ρ_0 and T_0 are a reference density and temperature, respectively. The constant β is the coefficient of thermal expansion: we expect that the density decreases as the temperature increases and so expect that $\beta > 0$.

In this section we shall make wide ranging use of the Boussinesq approximation (that variations in density are only important where they appear as a buoyancy term). We shall also assume that the specific heat capacities and densities of medium and fluid are the same, and that the temperatures are also equal (since any inhomogeneities at this microscopic scale would quickly be removed by thermal

diffusion). The temperature field within the porous medium is then described by the advection-diffusion equation

$$\frac{\partial T}{\partial t} + \mathbf{u} \cdot \nabla T = \kappa_T \nabla^2 T \tag{3.17}$$

where $\kappa_T = k/\rho c_p$ is the thermal diffusivity.

3.2.1 Linear instability calculation

We consider a porous layer of depth h heated to a uniform temperature $T_0 + \Delta T$ at the base and T_0 at the top. At a heuristic level, we expect that for sufficiently small ΔT it should be possible to maintain a static equilibrium: $\mathbf{u} = 0$, $\partial/\partial t = 0$. The heat equation (3.17) then requires that $\nabla^2 T = 0$ and so we have that

$$T_s = T_0 + \Delta T(1 - z/h),$$

to satisfy the boundary conditions at $z = 0$ and $z = h$. This thermal profile induces a density profile

$$\rho_s = \rho_0 \left[1 - \beta \Delta T(1 - z/h)\right]$$

so that there must also be a hydrostatic pressure profile

$$p_s = p_0 - \rho_0 g \left[z - \beta \Delta T(z - z^2/2h)\right].$$

We now consider small perturbations to this initial state,

$$\mathbf{u} = \mathbf{0} + \mathbf{u}', \quad T = T_s + T', \quad p = p_s + p'.$$

Noting the form of Darcy's law when the density varies, given by Eqn. (3.1), the equations of motion become

$$\nabla \cdot \mathbf{u}' = 0,$$

$$\mathbf{u}' = -\frac{k}{\mu} \left(\nabla p' + \rho' g \mathbf{e}_z\right) = -\frac{k}{\mu} \left(\nabla p' - \beta \rho_0 g T' \mathbf{e}_z\right),$$

and the linearized heat equation is

$$\frac{\partial T'}{\partial t} + \mathbf{u}' \cdot \nabla T_s = \kappa_T \nabla^2 T' = \frac{\partial T'}{\partial t} - w' \Delta T/h.$$

(Note that we are making use of the Boussinesq approximation in assuming that $\nabla \cdot \mathbf{u}' = 0$.)

We non-dimensionalize these equations by letting

$$(x, y, z) = h(X, Y, Z), \quad \mathbf{u}' = \frac{\kappa_T}{h}\mathbf{U}, \quad t = \frac{h^2}{\kappa_T}\tau, \quad p' = \frac{\mu \kappa_T}{k}P, \quad T' = \Delta T \, \Theta \tag{3.18}$$

so that we have

$$\nabla \cdot \mathbf{U} = 0, \tag{3.19}$$

$$\mathbf{U} = -\nabla P + \mathrm{Ra}\,\Theta\,\hat{\mathbf{e}}_{\mathbf{Z}}, \tag{3.20}$$

and

$$\frac{\partial \Theta}{\partial \tau} - W = \nabla^2 \Theta \tag{3.21}$$

where the *Rayleigh number*

$$\mathrm{Ra} = \frac{\beta \rho_0 g \Delta T k h}{\mu \kappa_T} \tag{3.22}$$

measures the buoyancy force relative to the dissipation (thermal and viscous).

We now need to analyse the system of equations (3.19)-(3.21). To simplify this, we first take the curl of (3.20) since we are then freed from having to determine the pressure perturbation P. Taking the curl again and using the result that $\nabla \wedge \nabla \wedge \mathbf{U} = -\nabla^2 \mathbf{U}$ since $\mathbf{U}$ is incompressible, we have

$$-\nabla^2 \mathbf{U} = \mathrm{Ra}\left(\Theta_{XZ}\hat{\mathbf{e}}_{\mathbf{X}} + \Theta_{YZ}\hat{\mathbf{e}}_{\mathbf{Y}} - \nabla_H^2 \Theta \hat{\mathbf{e}}_{\mathbf{Z}}\right), \tag{3.23}$$

where $\nabla_H^2 = \partial_X^2 + \partial_Y^2$ is the horizontal/planar Laplacian. In particular, by dotting with $\hat{\mathbf{e}}_{\mathbf{Z}}$ we find that

$$\nabla^2 W = \mathrm{Ra}\nabla_H^2 \Theta, \tag{3.24}$$

Note that equations (3.21) and (3.24) constitute two equations for the unknowns W and Θ and are to be solved subject to the boundary conditions

$$W = 0, \quad \Theta = 0 \tag{3.25}$$

on $Z = 0, 1$. Once these are determined we could, in principle, solve for the other velocity components and the pressure. guaranteed

To solve the problem (3.21), (3.24) and (3.25) we suppose a normal mode decomposition

$$W = \omega(Z)\exp\left(\sigma t + \mathrm{i}pX + \mathrm{i}qY\right), \quad \Theta = \vartheta(Z)\exp\left(\sigma t + \mathrm{i}pX + \mathrm{i}qY\right).$$

We then have the eigenvalue problem

$$\sigma\vartheta - \omega = \left(\frac{\mathrm{d}^2}{\mathrm{d}Z^2} - \alpha^2\right)\vartheta, \tag{3.26}$$

$$\left(\frac{\mathrm{d}^2}{\mathrm{d}Z^2} - \alpha^2\right)\omega = -\mathrm{Ra}\,\alpha^2\vartheta, \tag{3.27}$$

where $\alpha^2 = p^2 + q^2$, with boundary conditions

$$\omega(0) = \omega(1) = \vartheta(0) = \vartheta(1) = 0. \tag{3.28}$$

We see by inspection that a solution for the eigenvalue problem (3.26)-(3.27) is

$$\omega(Z) = \sin m\pi Z, \quad \vartheta(Z) = \frac{m^2\pi^2 + \alpha^2}{\alpha^2 \mathrm{Ra}}\sin m\pi Z \tag{3.29}$$

for some integer $m > 0$ (to avoid the trivial solution). The growth rate

$$\sigma = \frac{\text{Ra } \alpha^2}{m^2\pi^2 + \alpha^2} - m^2\pi^2 - \alpha^2 \tag{3.30}$$

Since σ is real, instability is characterised by $\sigma > 0$. We can see that σ decreases as the mode number m increases; therefore the value $m = 1$ gives the most unstable value of σ. Since σ increases with Ra, we see that $\sigma > 0$ (for $m = 1$) if $\text{Ra} > \text{Ra}_c(\alpha)$, where

$$\text{Ra}_c(\alpha) = \frac{(\pi^2 + \alpha^2)^2}{\alpha^2} \tag{3.31}$$

In turn, this value of the Rayleigh number depends on the selected value of α. Since an arbitrary disturbance will excite all wave numbers in the X and Y directions, it is the minimum value of $\text{Ra}_c(\alpha)$ that determines the absolute threshold for stability. The minimum of $\text{Ra}_c(\alpha)$ is obtained when $\alpha = \pi$ so that

$$\min_{\alpha} \text{Ra}_c(\alpha) = \text{Ra}_c(\pi) = 4\pi^2. \tag{3.32}$$

We therefore conclude that the static heated state is unstable if $\text{Ra} > 4\pi^2$. The detailed value of this instability threshold of course depends on the boundary conditions applied. However, the picture is qualitatively the same in these cases. The picture is also qualitatively similar for the heating of a thin layer of viscous liquid between two horizontal plates, although in this case the Rayleigh number becomes

$$\text{Ra} = \frac{\beta\rho_0 g\Delta T h^3}{\mu\kappa_T}, \tag{3.33}$$

which is the same as (3.22) for porous media with the permeability k replaced by the square of the layer thickness, h^2.

3.3 Double-diffusive convection

Double-diffusive convection refers to motion that is generated by buoyancy in the case where the density depends on two substances or quantities. The simplest example occurs when salt solutions are heated; in this case the two diffusing quantities are heat and salt. Double-diffusive processes occur in sea water, for example. Other simple examples occur in multi-component fluids containing more than one dissolved species; convection in magma chambers is one such.

The guiding principle behind double-diffusive convection is still that light fluid rises, and convection occurs in the normal way (the direct mode) when the steady state is statically unstable (i.e. when the density increases with height), but confounding factors arise when, as is normally the case, the two substances diffuse at different rates. This is a particularly important distinction when we are concerned with temperature and salt for two reasons: (i) the ratio of thermal to solutal diffusivity is large and (ii) an increase in temperature decreases the density while an increase in salt concentration increases the density. The two species are therefore acting in different directions. In this case different modes of convection occur near the statically neutral buoyancy state: the cells can take the form of

long thin "fingers" or the onset of convection can be oscillatory. In practice, fingers are seen, but oscillations are not.

A further variant on the purely thermal convection discussed in §3.2 arises in the form of convective layering. This is a long-lived transient form of convection, in which separately convecting layers form, and is associated partly with the high diffusivity ratio, and partly with the usual occurrence of no flux boundary conditions for diffusing chemical species.

We pose a model for double-diffusive convection based on a density which is related linearly to temperature T and salt composition C in the form

$$\rho = \rho_0[1 - \beta_T(T - T_0) + \beta_C(C - C_0)], \tag{3.34}$$

where we take solutal and thermal expansion coefficients β_C and β_T to be positive constants but have built into the equation of state the fact that the presence of salt makes the fluid heavier. In (3.34) C_0 is the (imposed) concentration of salt at the top of the layer, $z = h$.

The equation that then needs to be added to the equations used for thermal convection previously is that for convective diffusion of salt:

$$\frac{\partial C}{\partial t} + \mathbf{u} \cdot \nabla C = \kappa_C \nabla^2 C, \tag{3.35}$$

where κ_C is the solutal diffusion coefficient, assumed constant (although in practice it may also depend on the temperature).

We shall assume that, in addition to the boundary condition $C = C_0 + \Delta C$ at $z = 0$, we have $C = C_0$ at $z = h$. In the static situation then, we have temperature and concentration fields

$$T_s = T_0 + \Delta T(1 - z/h),$$

$$C_s = C_0 + \Delta C(1 - z/h)$$

to satisfy the boundary conditions at $z = 0$ and $z = h$. These thermal and solutal fields induce a density profile

$$\rho_s = \rho_0 \left[1 + (\beta_C \Delta C - \beta_T \Delta T)(1 - z/h)\right]$$

so that there must also be a hydrostatic pressure profile

$$p_s = p_0 - \rho_0 g \left[z + (\beta_C \Delta C - \beta_T \Delta T)(z - z^2/2h)\right].$$

We now consider small perturbations to this initial state,

$$\mathbf{u} = \mathbf{0} + \mathbf{u}', \quad T = T_s + T', \quad C = C_s + C', \quad p = p_s + p',$$

so that the equations of motion become

$$\nabla \cdot \mathbf{u}' = 0,$$

$$\mathbf{u}' = -\frac{k}{\mu} \left[\nabla p' + \rho_0 g(\beta_C C' - \beta_T T')\hat{\mathbf{e}}_{\mathbf{z}}\right].$$

The linearized equations for diffusion of heat and solute are, respectively,

$$\frac{\partial T'}{\partial t} + \mathbf{u}' \cdot \nabla T_s = \kappa_T \nabla^2 T' = \frac{\partial T'}{\partial t} - w' \Delta T/h.$$

and

$$\frac{\partial C'}{\partial t} + \mathbf{u}' \cdot \nabla C_s = \kappa_C \nabla^2 C' = \frac{\partial C'}{\partial t} - w' \Delta C / h.$$

We non-dimensionalize these equations in the same way as in §3.2.1 using (3.18). In addition we let

$$C' = \Delta C \chi$$

so that we have

$$\nabla \cdot \mathbf{U} = 0, \tag{3.36}$$

$$\mathbf{U} = -\nabla P + \left(\mathrm{Ra}\, \Theta - \frac{\mathrm{Ra}_s}{\mathrm{Le}} \chi \right) \hat{\mathbf{e}}_{\mathbf{z}}, \tag{3.37}$$

where

$$\mathrm{Ra}_s = \frac{\beta_C \rho_0 g \Delta C k h}{\mu \kappa_C} \tag{3.38}$$

is the *solutal Rayleigh number* measuring the buoyancy force relative to the dissipation (solutal and viscous) and

$$\mathrm{Le} = \frac{\kappa_T}{\kappa_C} \tag{3.39}$$

is the *Lewis number* measuring the relative diffusivity of solute and heat. Note also that

$$\mathrm{Ra}_s = \mathrm{Ra}\, \mathrm{Le} \times N$$

where

$$N = \frac{\beta_C \Delta C}{\beta_T \Delta T}. \tag{3.40}$$

We also have that

$$\frac{\partial \Theta}{\partial \tau} - W = \nabla^2 \Theta \tag{3.41}$$

and

$$\mathrm{Le}\left(\frac{\partial \chi}{\partial \tau} - W \right) = \nabla^2 \chi. \tag{3.42}$$

Proceeding in precisely the same way as in §3.2.1, we take the curl of (3.37) twice and use incompressibility to show that

$$\nabla^2 W = \mathrm{Ra}\left(\nabla_H^2 \Theta - N \nabla_H^2 \chi \right) \tag{3.43}$$

with ∇_H^2 again denoting the horizontal Laplacian. Note that (3.41)-(3.43) is a system of equations in the functions Θ, χ and W that is to be solved subject to the boundary conditions

$$W = \Theta = \chi = 0 \tag{3.44}$$

at $Z = 0, 1$.

By inspection, solutions satisfying the temperature and salinity equations are

$$W = \sin(m\pi Z) \exp\left(\sigma t + ipX + iqY\right) \tag{3.45}$$

$$\Theta = \frac{1}{\sigma + \alpha^2 + m^2\pi^2} \sin(m\pi Z) \exp\left(\sigma t + ipX + iqY\right), \tag{3.46}$$

$$\chi = \frac{\mathrm{Le}}{\sigma\mathrm{Le} + \alpha^2 + m^2\pi^2} \sin(m\pi Z) \exp\left(\sigma t + ipX + iqY\right), \tag{3.47}$$

where $\alpha^2 = p^2 + q^2$.

We substitute the solutions (3.45)-(3.47) into the governing equation (3.43) to obtain a quadratic in σ, which can be written in the form

$$A\sigma^2 + B\sigma + C = 0, \tag{3.48}$$

where

$$A = (\alpha^2 + m^2\pi^2)\mathrm{Le},$$

$$B = (\alpha^2 + m^2\pi^2)^2\left[1 + \mathrm{Le}\right] + \alpha^2\left(\mathrm{Ra}_s - \mathrm{Ra}\,\mathrm{Le}\right),$$

and

$$C = (\alpha^2 + m^2\pi^2)^3 + \left[\mathrm{Ra}_s - \mathrm{Ra}\right]\alpha^2(\alpha^2 + m^2\pi^2).$$

Instability occurs if either of the two roots of (3.48) has positive real part. Since Le is a property of the fluid, we take it as fixed and study the effect of varying Ra and Ra_s on the stability boundaries where $\mathrm{Re}(\sigma) = 0$. Firstly, if $\mathrm{Ra} < 0$ and $\mathrm{Ra}_s > 0$, then A, B and C are all positive. From this it follows simply that $\mathrm{Re}(\sigma) < 0$ and we conclude that when both temperature and salinity fields are stabilizing, the state of no motion is linearly stable.

To find regions of instability in the $(\mathrm{Ra}_s, \mathrm{Ra})$ plane, it suffices to locate the curves where $\mathrm{Re}(\sigma) = 0$. There are two possibilities:

Exchange of stability (Direct mode)   One possibility is that $\mathrm{Re}(\sigma) = 0$ occurs when $\sigma = 0$. From (3.48), this is when $C = 0$, or $\mathrm{Ra}_s = \mathrm{Ra} - (\alpha^2 + m^2\pi^2)^2/\alpha^2$. For each value of α, this is a single curve and since we know that $\mathrm{Re}(\sigma) < 0$ in $\mathrm{Ra} < 0$ and $\mathrm{Ra}_s > 0$, this immediately tells us that a direct instability occurs if

$$\mathrm{Ra} - \mathrm{Ra}_s > \min_\alpha \frac{(\alpha^2 + \pi^2)^2}{\alpha^2} = 4\pi^2. \tag{3.49}$$

This direct transition is the counterpart of the onset of purely thermal convection (§3.2), and shows that $\mathrm{Ra} - \mathrm{Ra}_s$ is the effective Rayleigh number.
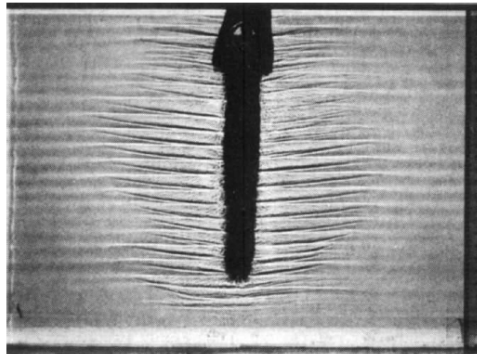
Fig. 2 Shadowgraph photograph showing the tilted layers and interfaces produced by inserting a block of ice into salt-stratified water at room temperature. (Specific gravity at top of tank 1.00, and at bottom 1.05; depth 26 cm.)

Figure 3.2: Experimental observation of the formation of double-diffusive fingers caused by melting of an ice block in salty water (with salt stratification). Taken from Huppert and Turner, *Nature* **271**, 46 (1978).

Hopf bifurcation   The other way in which $\mathrm{Re}(\sigma) = 0$ is for the complex conjugates values of σ to cross the imaginary axis at $\pm i\Omega$, say. See the example sheet for further details.

The geophysical relevance of these instabilities can be found J. S. Turner, *Buoyancy Effects in Fluids*, CUP. There it is noted that the observation of oscillatory instability is generally rare. Furthermore, a characteristic feature of 'double-diffusive' convection is that the direct mode instability develops into finger-like structures. An example of this is shown in figure 3.2 for the case of a pure ice block melting in salty water. The fact that these fingers propagate roughly horizontally (rather than the melt water rushing upwards without mixing, as one might expect) is one reason why the idea of supplying fresh water to dry countries by towing icebergs and siphoning off the melt water is not feasible! See Huppert and Turner, *Nature* **271**, 46 (1978) for more discussion.

3.4   Horizontal gravity-driven flows

Variations in buoyancy usually give rise to vertical flows, as studied in the last section of thermal convection. However, as we saw with droplet spreading in §2.2.3 the presence of an impermeable boundary allows vertical density differences to drive horizontal flows. Here we shall consider the problem of a finite volume V of fluid with density ρ released above an impermeable boundary within a porous medium. This is the porous medium analogue of the droplet spreading problem considered in §2.2.3 neglecting the effect of surface tension, which is an extremely complicated problem for flow in porous media.

3.4.1   Long, thin flows

We begin by considering the scaling behaviour of Darcy's law for an axisymmetric flow with typical vertical scale H and radial scale R such that $\delta = H/R \ll 1$. The velocity within the porous medium

$\mathbf{u} = (u, w)$ has typical scales $u \sim U$, $w \sim W$ where conservation of mass tells us that

$$\frac{W}{H} \sim \frac{1}{R^2} \times RU \implies W \sim \delta U.$$

Considering the horizontal component of Darcy's law we have that

$$\frac{\partial p}{\partial r} = -\frac{\mu}{k} u \implies P \sim \frac{\mu}{k} RU$$

where P is the typical scale for pressure. Looking at the terms that appear in the vertical component of Darcy's law we notice that

$$\frac{\mu W/k}{\partial p/\partial z} \sim \frac{\mu W/k}{P/H} \sim \frac{\mu \delta U/k}{\mu RU/kH} \sim \delta^2 \ll 1.$$

The vertical component of Darcy's law therefore gives that

$$\frac{\partial p}{\partial z} \approx -\rho g \tag{3.50}$$

so that the pressure is approximately hydrostatic, just as we found for lubrication theory in §2.2. While the idea presented here as well as the result are very similar to what we saw in lubrication theory, purists prefer to talk of the approximation made here as a 'long wavelength approximation' (rather than the lubrication approximation).

3.4.2   Porous medium gravity currents

For simplicity, we shall consider the problem of a drop of fluid of density ρ, volume V released within a porous medium bounded below by an impermeable boundary. Just as for a droplet released on a flat plate in the absence of a porous medium, we anticipate that the liquid will spread out horizontally along the boundary and will at late times satisfy the long wavelength assumption made above. We would like to calculate the evolution of the current profile $z = h(r, t)$ at late times and, in particular, the radial extent of the drop profile, $s(t)$, where $h(s(t), t) = 0$ for $s > s(t)$. To do this, we begin with (3.50), which may be integrated once to give

$$p = p_a + \rho g \big[h(r, t) - z \big] \tag{3.51}$$

where p_a is the pressure outside the drop and assumed to be atmospheric.

Now examining the horizontal component of Darcy's law, we find that the horizontal velocity component is

$$u = -\frac{k}{\mu} \frac{\partial p}{\partial r} = -\frac{k \rho g}{\mu} \frac{\partial h}{\partial r}. \tag{3.52}$$

We note that this horizontal velocity is independent of z and so $\bar{u} = u$. Being careful to incorporate the porosity ϕ into the equation of conservation of mass, we have that local continuity gives

End lecture 7

$$\phi \frac{\partial h}{\partial t} = -\frac{1}{r} \frac{\partial}{\partial r} (ruh) = \frac{k \rho g}{\mu r} \frac{\partial}{\partial r} \left(rh \frac{\partial h}{\partial r} \right). \tag{3.53}$$

The nonlinear diffusion equation (3.53) is to be solved together with the global conservation of mass, which may be written

$$V = 2\pi\phi \int_0^{s(t)} rh \, \mathrm{d}r. \tag{3.54}$$

We non-dimensionalize (3.53)-(3.54) with the length scale $(V/\phi)^{1/3}$ and time scale $(\phi^2 V)^{1/3}\mu/k\rho g$. We must then solve

$$\frac{\partial H}{\partial T} = \frac{1}{R}\frac{\partial}{\partial R}\left(RH\frac{\partial H}{\partial R}\right) \tag{3.55}$$

subject to

$$2\pi \int_0^{S(T)} RH \, \mathrm{d}R = 1 \tag{3.56}$$

and $H(S(T), T) = 0$.

   We would like to find the long time behaviour of the system (3.55)-(3.56) and so look for a similarity solution. With a similarity variable η given by

$$R = \eta T^\alpha,$$

and with a similarity solution of the form

$$H(R, T) = T^{-\beta}\chi(\eta)$$

we have

$$-\frac{1}{T^{\beta+1}}\left[\beta\chi + \alpha\eta\frac{\mathrm{d}\chi}{\mathrm{d}\eta}\right] = \frac{1}{T^{2(\alpha+\beta)}}\frac{1}{\eta}\frac{\mathrm{d}}{\mathrm{d}\eta}\left[\eta\chi\frac{\mathrm{d}\chi}{\mathrm{d}\eta}\right]. \tag{3.57}$$

Thus we take $2\alpha + \beta = 1$. In the limit $\phi \to 1$, $g \to 0$ we have a quasi-static drop that should be equivalent in shape to the small surface tension limit of the radial drop solution of Eqn. (2.36), i.e.

$$h(r) = A(r_0^2 - r^2),$$

noting this is valid for general capillary number, Ca. Here, changes in ϕ, g just change the timescale and not the drop-shape and thus away from these limits we still have the same shape here. From Eqn. (2.36) we thus require $H(R, T) \sim A_0(R_0^2 - R^2)$ after a sufficiently long time for transients to settle. Hence we seek a solution for χ of the form

$$\chi = A(\eta_0^2 - \eta^2),$$

where A, η_0 are independent of η. Substituting this into Eqn. (3.57) for $2\alpha + \beta = 1$ gives a solution once

$$A = \frac{1}{8}, \quad \alpha = \frac{1}{4}, \quad \beta = \frac{1}{2}.$$

The value of η_0, which determines the spread of the drop, is itself determined from the similarity form of (3.56). Noting $S(T)$ inherits the same similarity scaling as R, so that $S(T) = \eta_0 T^\alpha$, we have

$$1 = 2\pi \int_0^{\eta_0} \eta \chi \ \mathrm{d}\eta = \frac{\pi}{16} \eta_0^4.$$

Hence $\eta_0 = 2/\pi^{1/4}$ and the radius of the drop for late times $T \gg 1$ is given by

$$S(T) = \eta_0 T^\alpha = \frac{2}{\pi^{1/4}} T^{1/4}. \tag{3.58}$$

We have assumed in this calculation that the porous medium is initially dry. In reality would have to worry about surface tension etc. However, many flows of interest involve injecting a fluid of one density into a porous medium saturated with a liquid of close but not identical density. This may substantially alleviate the problems caused by surface tension at the pore scale. If, in addition, the porous medium is effectively unbounded then the flow outside the current may be neglected and the analysis above may be carried through with the density ρ replaced by the density difference $\Delta\rho$. It is more common in such scenarios that injection will continue indefinitely so that $V \propto t$ rather than being constant. In this case $r \sim t^{1/2}$ (see problem sheet) — a result that is useful in predicting the rate of spreading of carbon dioxide when it is pumped into geological aquifers for carbon sequestration to mitigate the effects of climate change. More details of this topical application can be found in M. Bickle *et al.*, *Earth Planet. Sci. Lett.* **255**, 164 (2007).

4 Biofluid flows: Cilia and Flagella

In this section we will first consider aspects of bio-fluid dynamics at the level of cell, and focus on fluid actuation and cell swimming by the movement of slender cellular appendages, in particular cilia and flagella.

4.1 Characteristic Equations and Scales for Cellular Swimming

The non-dimensional Navier Stokes equations are

$$\text{Re}\left(\frac{\partial \boldsymbol{u}'}{\partial t'} +\ \boldsymbol{u}' \cdot \nabla' \boldsymbol{u}'\right) = -\nabla p + \nabla^2 \boldsymbol{u}, \quad \text{Re} = \frac{\rho U L}{\mu}.$$

For most eukaryotic cells (i.e. excluding bacteria), typical scales are $L \sim 10\mu$m, and $U \sim 100\mu$ms^{-1} for the cell swimming speed (or ciliary fluid propulsion speeds); also $\rho/\mu \sim 10^6$ SI units for water. Hence

$$\text{Re} \sim 10^{-3}$$

and one can safely neglect the inertial terms. Bacteria swim with even smaller Reynolds numbers. Thus, for cellular fluid dynamics, we work with Stokes' equations

$$\nabla \cdot \boldsymbol{u} = 0, \quad 0 = -\nabla p + \mu \nabla^2 \boldsymbol{u}. \tag{4.1}$$

In addition, most cells are neutrally buoyant, so that gravity and buoyancy cancel and we assume this throughout.

4.1.1 Force and torque free swimming

The equation of motion for its centre of mass $\boldsymbol{x}$ is given by

$$M\ddot{\boldsymbol{x}} = \int_{Swimmer} \boldsymbol{\sigma} \cdot \boldsymbol{n} \mathrm{d}S,$$

where $\boldsymbol{\sigma} \sim \mu U/L$ is the stress tensor associated with the fluid movement. The lengthscale L is the lengthscale of the swimmer and the swimmer's density is that of the fluid as it is neutrally buoyant. Hence the ratio of the scale of the inertial term $M\ddot{\boldsymbol{x}}$ to the fluid force, R_S, and referred to as the Stokes number, is given by

$$\text{R}_S \sim \frac{(\rho L^3)(L/T^2)}{\mu \dfrac{U}{L} L^2} \sim \frac{\rho}{\mu} U L = \text{Re},$$

where $T \sim L/U$ is the timescale of the flow. Hence, to an excellent approximation, there is not net force on a neutrally buoyant swimmer in Stokes flow. A similar argument shows there is no net torque.

4.1.2 Boundary conditions for Swimmers and Cilia

Conditions at infinity If the modelling approximation includes an infinite domain, one must specify the velocity at infinity as part of the boundary conditions:

$$\boldsymbol{u}(\boldsymbol{x}, t) \to \boldsymbol{u}_\infty(\theta, \varphi, t) \quad \text{as } |\boldsymbol{x}| \to \infty, \tag{4.2}$$

where θ, φ are spherical polar angles. Often, but not always, $\boldsymbol{u}_\infty = 0$.

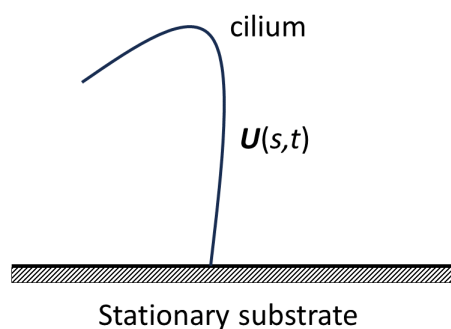**Cilia on an underlying substrate, e.g. lung cilia**

Figure 4.1: A cilium with velocity profile $\boldsymbol{U}(s, t)$.

With s arclength along a cilium and t time, as depicted in Fig.4.1, typically one imposes the cilia beat in which case the boundary conditions on the cilium are $\boldsymbol{u} = \boldsymbol{U}(s, t)$, with $\boldsymbol{u} = \boldsymbol{0}$ on the underlying substrate. This implicitly assumes the cilium is very thin, with a radius much less than the radius of curvature of its centreline, so that its surface velocity is effectively equal to that of its centreline.

A swimmer
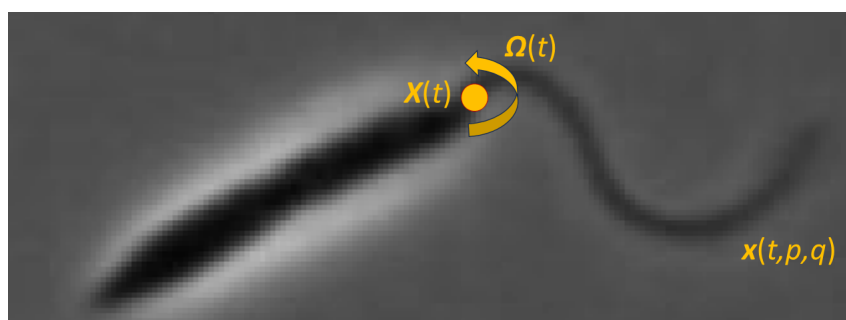
Figure 4.2: A swimming cell, *Leishmania major*, with its surface parameterised as $\boldsymbol{x}(t, p, q)$, where p, q are surface coordinates. Let $\boldsymbol{X}(t)$ given the position vector of a body fixed point, with $\boldsymbol{U}(t) = \dot{\boldsymbol{X}}(t)$ and let $\boldsymbol{\Omega}(t)$ denote the angular velocity of the swimmer about this point. The bright halo around the cell body is an optical artefact of phase contrast microscopy.

As shown in Fig.4.2, let $\boldsymbol{X}(t)$ denote the position vector of a body fixed point, with $\boldsymbol{U}(t) = \dot{\boldsymbol{X}}(t)$ its velocity and $\boldsymbol{\Omega}(t)$ denote the angular velocity of the swimmer about $\boldsymbol{X}(t)$. In addition, let $\boldsymbol{x}(t, p, q)$ parameterise the surface at time t, where p, q are surface coordinates. Then we have the boundary conditions on the cell surface

$$\boldsymbol{u}(t, p, q) = \boldsymbol{U}(t) + (\boldsymbol{x}(t, p, q) - \boldsymbol{X}(t)) \wedge \boldsymbol{\Omega}(t) + \left\{ \begin{array}{ll} \boldsymbol{u}_{flagellum}(t, p, q) & \boldsymbol{x}(t, p, q) \in \quad \text{Flagellum} \\ \boldsymbol{0} & \boldsymbol{x}(t, p, q) \in \quad \text{Cell Body} \end{array} \right.$$

(4.3)

Here $\boldsymbol{u}_{flagellum}(t, p, q)$ is the velocity of the flagellum in the reference frame translating and rotating with the cell and is assumed known – for example Leishmania flagella have sinusoidal travelling waves in the cell-fixed frame to good approximation. Often $\boldsymbol{u}_{flagellum}(t, p, q)$ will be simplified to $\boldsymbol{u}_{flagellum}(t, s)$, where s is arclength along the flagellum, so that the flagella surface moves at the same speed as its centreline, which is an excellent approximation for a thin filament, with radius much less than the radius of curvature of the centreline.

However, $\boldsymbol{U}(t)$, $\boldsymbol{\Omega}(t)$ are not known a priori. These 6 scalar unknowns are fixed by the 6 scalar conditions given the absence of forces and torques on the body:

$$\int_{Swimmer} \boldsymbol{\sigma} \cdot \boldsymbol{n} \, \mathrm{d}S = \boldsymbol{0}, \qquad \int_{Swimmer} (\boldsymbol{x}(t, p, q) - \boldsymbol{X}(t)) \wedge \boldsymbol{\sigma} \cdot \boldsymbol{n} \mathrm{d}S = \boldsymbol{0}.$$

Note it is legitimate to resolve the torque about the body fixed point $\boldsymbol{X}(t)$ rather than the centre of mass or a point fixed in an inertial frame as the swimmer is force free and hence

$$\int_{Swimmer} \boldsymbol{X}(t) \wedge \boldsymbol{\sigma} \cdot \boldsymbol{n} \mathrm{d}S = \boldsymbol{X}(t) \wedge \int_{Swimmer} \boldsymbol{\sigma} \cdot \boldsymbol{n} \mathrm{d}S = \boldsymbol{0}.$$

Thus the general swimmer problem is very difficult, though there are many simplifying approximations. Below, we will exploit the slenderness of the *Leishmania major* cell to simplify the problem.

4.2   Purcell's Scallop theorem

Purcell's Scallop Theorem. In Stokes flow, a swimmer exhibiting reciprocal motion has no net movement.

It is called the scallop theorem because a scallop, with its single hinge, thus cannot swim in the Stokes flow regime. A scallop of course can swim as it is sufficiently large for inertial effects to be important. The scallop theorem provides a significant constraint to the means by which cells, or artificial microdevices, can swim or pump fluid.

> **Proving Purcell's Scallop Theorem for a flagellated cell with a reciprocal beat.**
>
> The cell is driven by its flagellar beating. Suppose its beating is reciprocal so that
>
> $$\boldsymbol{u}_{flagellum}(t,p,q) = \boldsymbol{v}(t,p,q), \quad t \in [0,T]; \quad \boldsymbol{u}_{flagellum}(t,p,q) = -\boldsymbol{v}(2T-t,p,q), \quad t \in [T,2T].$$
>
> and the flagellum exactly reverses it motion in the cell-fixed frame in the second half of the beat. Then writing the solution for the Stokes equation as
>
> $$\nabla p(t,\boldsymbol{x}), \quad \boldsymbol{u}(t,\boldsymbol{x}), \quad \boldsymbol{U}(t), \quad \boldsymbol{\Omega}(t)$$
>
> for $t \in [0,T]$ then linearity and the absence of time derivatives entails
>
> $$-\nabla p(2T-t,\boldsymbol{x}), \quad -\boldsymbol{u}(2T-t,\boldsymbol{x}), \quad -\boldsymbol{U}(2T-t), \quad -\boldsymbol{\Omega}(2T-t)$$
>
> is a solution of the Stokes equations for $t \in [T,2T]$. Noting solutions to Stokes equations with velocity boundary conditions are unique up to an additive constant in the pressure (see e.g. Chapter 1 of [4]), this is the solution. Hence $\boldsymbol{U}(t) = -\boldsymbol{U}(2T-t)$ by uniqueness and the net displacement of the cell is
>
> $$\int_0^T \boldsymbol{U}(t)\mathrm{d}t + \int_T^{2T} \boldsymbol{U}(a)\mathrm{d}a = \int_0^T \boldsymbol{U}(t) + \boldsymbol{U}(2T-t)\mathrm{d}t = \boldsymbol{0},$$
>
> where the substitution $t = 2T-a$ is used in the integration. Thus the cell makes no net progress.
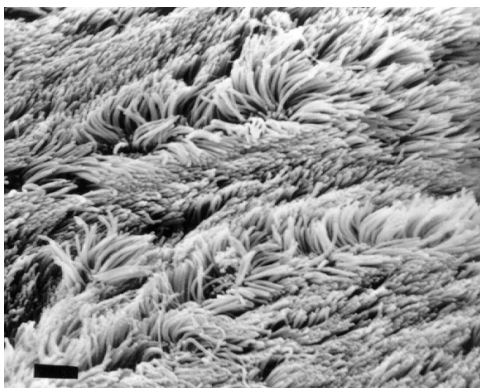
4.3   Ciliary Pumping

Figure 4.3: An image of cilia from rabbit trachea. Note how close the cilia are spaced; to give an idea of scale the length of a cilium is about 6 microns.

Cilia line most of the surface area of the airways (Fig.4.3), where they beat in a coordinated manner as. The beating of an individual cilium relative to its nearest neighbour is slightly out of phase, and
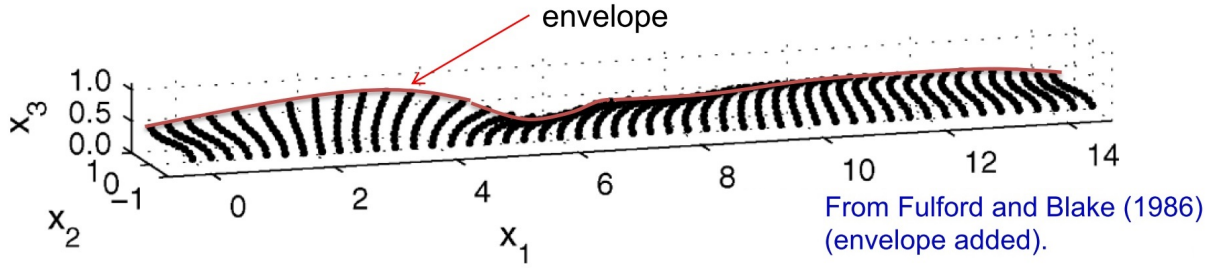
Figure 4.4: Ciliary beating on the surface of the lung forms a wave, denoted the metachronal wave. In the simplest model, the envelope of this wave is considered as an undulating, impermeable sheet. A fundamental question is: what speed is the fluid above the cilia pumped at for a given time-dependent deformation of the envelope geometry.

hence a long wavelength metachronal wave is formed; see Fig. 4.4. Given how close respiratory tract cilia are placed, as seen in Fig. 4.3, a common assumption is model the envelope of cilia tips as an impermeable surface, generating the envelope model. The fundamental question we address is, given the metachronal wave movement, how fast is the fluid pumped by the cilia? This was originally addressed by Blake [1].

4.3.1   A mathematical model of ciliary pumping

We non-dimensionalise length with respect to the inverse wavenumber of the metachronal wave, k^{-1}, time with respect to the inverse frequency, ω^{-1} and velocity with respect to the scale ωk^{-1}. The non-dimensional equations for the fluid are

$$\nabla \cdot \boldsymbol{u} = 0, \quad 0 = -\nabla p + \nabla^2 \boldsymbol{u}. \tag{4.4}$$

We further simplify. The envelope wave amplitudes are taken to be small relative to k^{-1}, single frequency, and $\pi/2$ out of phase, with x along the lung surface assumed flat, y perpendicular to the lung surface and homogeneity in the third direction. With the y coordinate such that the plane $y = 0$ coincides with the mid plane of the metachronal wave, and noting the non-dimensionalisation, the envelope of the metachronal wave is then given by

$$x_e = x + \epsilon a \cos(x - t), \qquad y_e = \epsilon b \sin(x - t),$$

with $\epsilon \ll 1$ by the small wave amplitude assumption. Thus with $\boldsymbol{u} = (u, v)$, we have the boundary condition

$$u(x_e, y_e) = \frac{\partial x_e}{\partial t} = \epsilon a \sin(x - t), \qquad v(x_e, y_e) = \frac{\partial y_e}{\partial t} = -\epsilon b \cos(kx - t),$$

We also have

$$(u, v) \to (U, 0) \ \text{ as } \ y \to \infty,$$

where U is a priori unknown, and the fundamental quantity we seek, but must be found as part of the solution.

Since $\nabla \cdot \boldsymbol{u} = 0$, we can express $\boldsymbol{u}$ via the streamfunction

$$u = \frac{\partial \psi}{\partial y}, \qquad v = -\frac{\partial \psi}{\partial x}.$$

Fundamental equations for ψ, U. Taking the curl of the momentum equation we have

$$\nabla^4 \psi = 0$$

with

$$\frac{\partial \psi}{\partial y}(x_e, y_e) = \epsilon a \sin(x - t), \qquad \frac{\partial \psi}{\partial x}(x_e, y_e) = \epsilon b \cos(kx - t),$$

$$x_e = x + \epsilon a \cos(x - t), \qquad y_e = \epsilon b \sin(x - t), \qquad (\psi_y, \psi_x) \to (U, 0) \quad \text{as} \quad y \to \infty.$$

Solution We seek a perturbative solution. Clearly if $\epsilon = 0$ the solution is $U = \psi = 0$ as nothing is driving the flow. Hence we write

$$\psi = \epsilon \psi_1(x, y) + \epsilon^2 \psi_2(x, y) + O(\epsilon^3), \qquad U = \epsilon U_1 + \epsilon^2 U_2 + O(\epsilon^3), \ .$$

Finding ψ_1, U_1.

At $O(\epsilon)$ we have

$$\nabla^4 \psi_1 = 0$$

$$\psi_{1y}(x, 0) = a \sin(x - t), \quad \psi_{1x}(x, 0) = b \cos(x - t), \quad \psi_{1y}(x, \infty) = U_1, \quad \psi_{1x}(x, \infty) = 0.$$

Let $\psi_1 = f(y) \sin(x - t)$. Then

$$0 = \nabla^4 \psi_1 = [f'''' - 2f'' + f] \sin(x - t)$$

and hence

$$f = Ae^{-y} + Be^y + Cye^{-y} + Dye^y,$$

where A, B, C, D are constant. To avoid blow up as $y \to \infty$ we have $B = D = 0$ and thus

$$\psi_1(x, y) = (A + Cy)e^{-y} \sin(x - t), \qquad \psi_{1y}(x, y) = (-A - Cy + C)e^{-y} \sin(x - t).$$

From the condition $\psi_{1x}(x, 0) = b \cos(x - t)$ we have $A = b$ and the condition

$$\psi_{1y}(x, 0) = a \sin(x - t)$$

gives $C - A = C - b = a$ and hence $C = a + b$. Hence we find

$$\psi_1 = (b + (a + b)y)e^{-y} \sin(x - t), \tag{4.5}$$

and since $\psi_{1y} \to 0$ as $y \to \infty$, we have $U_1 = 0$ and there is no pumping at this order.

Hence, we must go to second order to find the leading order pumping speed.

Finding U_2.

We first of all consider the boundary conditions at next order. The condition

$$\frac{\partial \psi}{\partial y}(x_e, y_e) = \epsilon a \sin(x - t), \quad x_e = x + \epsilon a \cos(x - t), \quad y_e = \epsilon b \sin(x - t), \quad \psi = \epsilon \psi_1 + \epsilon^2 \psi_2 + \dots$$

gives at $O(\epsilon^2)$ that

$$a \cos(x - t)\psi_{1yx}(x, 0) + b \sin(x - t)\psi_{1yy}(x, 0) + \psi_{2y}(x, 0) = 0. \tag{4.6}$$

Similarly, from

$$\frac{\partial \psi}{\partial x}(x_e, y_e) = \epsilon b \cos(kx - t)$$

we have

$$a \cos(x - t)\psi_{1yx}(x, 0) + b \sin(x - t)\psi_{1yy}(x, 0) + \psi_{2y}(x, 0) = 0. \tag{4.7}$$

Using Eqn. (4.5) we have

$$\psi_{2y}(x, 0) = -a^2 \cos^2(x - t) + b(b + 2a)\sin^2(x - t) = \frac{b^2 + 2ab - a^2}{2} - \frac{(b + a)^2}{2}\cos(2(x - t)),$$

$$\psi_{2x}(x, 0) = 0.$$

By linearity, we can consider the terms contributing to $\psi_{2y}(x, 0)$ separately. Further the contribution

$$-\frac{1}{2}(b + a)^2 \cos(2(x - t))$$

will generate a contribution to ψ_2 that will oscillate sinusoidally and thus will not generate net pumping. In fact, analogously to the solution for ψ_1, one can show this contribution to ψ_2 scales as

$$\psi_2 \sim y e^{-4y}$$

and thus this will not contribute to U_2 even in a sinusoidal manner. Hence we only consider the contribution to ψ_2, denoted η, that solves

$$\nabla^4 \eta = 0$$

$$\eta_y(x, 0) = \tfrac{1}{2}(b^2 + 2ab - a^2), \quad \eta_x(x, 0) = 0, \quad \lim_{y \to \infty} \eta_y(x, y) = U_2, \quad \lim_{y \to \infty} \eta_x(x, y) = 0.$$

There is no $x-$dependence in the inhomogeneous driver, $(b^2 + 2ab - a^2)/2$, so we take $\eta = \eta(y)$. Also η is a streamfunction contribution so η can be changed by an additive constant without changing the physics, so we impose $\eta(0) = 0$ without loss. We also require η_y does not blow up at infinity so that flows are finite. Solving with these constraints, on noting $\nabla^4 \eta = 0$ reduces to

$$\frac{\mathrm{d}^4 \eta}{\mathrm{d}y^4} = 0,$$

gives

$$\eta(y) = \frac{1}{2}(b^2 + 2ab - a^2)y$$

and hence

$$\epsilon^2 U_2 = \epsilon^2 \lim_{y \to \infty} \eta_y = \frac{\epsilon^2}{2}(b^2 + 2ab - a^2)$$

is the leading order approximation for the non-dimensional speed that the cilia are predicted to pump the fluid in the far field.

4.4   Simple observations about, and solutions for, Stokes' equations

Before we consider cellular motility in detail, we consider some observations about, and solutions for, Stokes flow.

4.4.1   The Stokeslet.

The Stokeslet is the Stokes flow for a point forcing located at $\boldsymbol{x}_0$. It can be obtained by considering the Stokes equations for a point force $\boldsymbol{m}$ located at $\boldsymbol{x} = \boldsymbol{x}_0$:

$$-\nabla p + \mu \nabla^2 \boldsymbol{u} + \boldsymbol{m}\delta(\boldsymbol{x} - \boldsymbol{x}_0) = \boldsymbol{0}, \quad \nabla \cdot \boldsymbol{u} = 0, \tag{4.8}$$

with no flow or pressure gradient at infinity,

$$\nabla p, \;\; \boldsymbol{u} \to \boldsymbol{0} \quad \text{as} \;\; |\boldsymbol{x}| \to \infty.$$

With $\hat{\boldsymbol{x}} = \boldsymbol{x} - \boldsymbol{x}_0$ and $r = |\boldsymbol{x} - \boldsymbol{x}_0|$ the Stokeslet is given by

$$u_i = \frac{1}{8\pi\mu} G_{ij} m_j, \tag{4.9}$$

where

$$G_{ij} = \frac{\delta_{ij}}{r} + \frac{\hat{x}_i \hat{x}_j}{r^3}.$$

This is also known as the Oseen-Burgers tensor or the free-space Greens function.

Derivation of the Stokeslet

By translational invariance we take, without loss, $\boldsymbol{x}_0 = \boldsymbol{0}$. By linearity

$$u_i = \frac{1}{\mu} K_{ij} m_j$$

where K_{ij} is a rank-2 tensor, with no further dependence on μ or $\boldsymbol{m}$ and thus it depends on $\boldsymbol{x}$ only as there are no other parameters in the equations; one can also readily show that $\boldsymbol{K}$ has dimensions of inverse length.

We note a useful representation of the delta-function:

$$\delta(\boldsymbol{x}) = -\frac{1}{4\pi} \nabla^2 \left(\frac{1}{r} \right).$$

Taking the divergence of Eqn. (4.8) and using fluid incompressibility we have

$$-\nabla^2 p + \boldsymbol{m} \cdot \nabla \left(-\frac{1}{4\pi} \nabla^2 \left(\frac{1}{r} \right) \right) = 0.$$

Noting $\nabla p \to \boldsymbol{0}$ as $|\boldsymbol{x}| \to \infty$, we have

$$p = -\frac{1}{4\pi} \boldsymbol{m} \cdot \nabla \left(\frac{1}{r} \right),$$

and, without loss, fixing the additive constant freedom in the pressure to be zero. Substituting back into Eqn. (4.8) we have

$$\mu \nabla^2 \boldsymbol{u} = \frac{\boldsymbol{m}}{4\pi} \nabla^2 \left(\frac{1}{r} \right) - \frac{1}{4\pi} \nabla \left(\boldsymbol{m} \cdot \nabla \left(\frac{1}{r} \right) \right).$$

Using summation convention and noting $\boldsymbol{m}$ is constant this gives

$$\mu \nabla^2 u_i = \frac{m_j}{4\pi} \left[\delta_{ij} \nabla^2 - \frac{\partial^2}{\partial x_i \partial x_j} \right] \frac{1}{r}. \tag{4.10}$$

Let

$$u_i = \frac{1}{\mu} \frac{m_j}{4\pi} \left[\delta_{ij} \nabla^2 - \frac{\partial^2}{\partial x_i \partial x_j} \right] G(r), \tag{4.11}$$

where $\nabla^2 G = 1/r$. Noting the derivatives commute, the expression of Eqn.(4.11) solves Eqn.(4.10) and is divergenceless.

Solving for a particular solution of $G(r)$,

$$\frac{1}{r} = \nabla^2 G = \frac{1}{r}(rG)'',$$

so that we can take $G = r/2$; we will return to homogeneous solutions of the Laplacian and the fact this means G is not unique. With $G = r/2$ we have

$$u_i = \frac{1}{\mu} \frac{m_j}{4\pi} \left[\delta_{ij} \nabla^2 - \frac{\partial^2}{\partial x_i \partial x_j} \right] \frac{r}{2} = \frac{1}{8\pi\mu} \left(\frac{\delta_{ij}}{r} + \frac{\hat{x}_i \hat{x}_j}{r^3} \right) m_j. \tag{4.12}$$

To reinstate the $\boldsymbol{x}_0$ dependence, simply replace $\boldsymbol{x} \to \boldsymbol{x} - \boldsymbol{x}_0$, generating the Stokeslet solution.

Lack of uniqueness of G. There are other possible contributions to G. Noting G can scale at most like r else the resulting contribution to u_i will blow up at infinity, these contributions scale like

$$G \sim r^n,$$

where n is integer, as may be readily deduced from the separable solution of Laplace's equation in spherical polars. For $n = 1$ the constant term and the homogeneous solutions for G terms any linear sum of $x = x_1$, $y = x_2$ and $z = x_3$. However, this would be annihilated by the operator

$$\left[\delta_{ij} \nabla^2 - \frac{\partial^2}{\partial x_i \partial x_j} \right]$$

and thus does not contribute to u_i. Note $[G] = L$ for the expression for u_i to be dimensionally correct. For $G \sim r^n$, $n \neq 1$, a scalar constant is required of dimension L^{1-n} for the contribution to u_i to be dimensionally correct. However, there are no terms from the model parameters with this dimension, and generating a scalar term with the correct dimension from $\boldsymbol{x}$ will use powers of r and thus regenerate $G \sim r$, which has been already covered. Thus no other solutions are generated from the lack of uniqueness for G.

4.4.2   The potential dipole and the point source dipole

As Stokes' equation are linear and hence we can build up solutions by the linear superposition of solutions, such as the Stokeslet, which have point forces outside the domain, in direct analogy to the method of images for the solution of problems in electrostatics, or Laplace's equation for example.

The potential solution Other solutions of Stokes equations are useful this purpose too. The simplest, known as the potential dipole, has constant pressure, with the velocity

$$u_i = -\frac{\partial}{\partial x_i}\left(\frac{1}{r}\right) = \frac{\hat{\boldsymbol{x}}}{r^3},$$

given by the gradient of a potential, where once more $\hat{\boldsymbol{x}} = \boldsymbol{x} - \boldsymbol{x}_0$ and $r = |\boldsymbol{x} - \boldsymbol{x}_0|$.

Excluding $\boldsymbol{x} = \boldsymbol{x}_0$ from the domain, this is divergence-free as

$$\nabla \cdot \boldsymbol{u} \sim \nabla^2\left(\frac{1}{r}\right),$$

with right-handside a delta-function that is zero away from $\boldsymbol{x} = \boldsymbol{x}_0$. Similarly

$$\nabla^2 u_i = 0$$

by similar reasoning and hence the Stokes equation is satisfied.

The point source dipole, potential dipole Because the only boundary constraint is decay at infinity, one can differentiate the above solutions with respect to the location of the singularity, $\boldsymbol{x}_0$, to generate a further solution. Thus with

$$D_{ij} = -\frac{\partial}{\partial x_{0,j}}\left(\frac{\hat{\boldsymbol{x}}}{r^3}\right) = -\frac{\delta_{ij}}{r^3} + 3\frac{\hat{x}_i \hat{x}_j}{r^5}$$

we have

$$u_i = D_{ij}q_j$$

is a solution of Stokes equations for any constant vector $\boldsymbol{q}$, noting the incompressibility condition is also inherited.

4.4.3   The solution for a translating sphere

Consider the Stokes equations for a neutrally buoyant sphere of radius a translating at constant speed $\mathbf{U}$ in the absence of other boundaries. The governing equations are

$$-\nabla p + \mu \nabla^2 \boldsymbol{u} = \boldsymbol{0}, \quad \nabla \cdot \boldsymbol{u} = 0 \quad \text{for} \quad |\boldsymbol{x} - \boldsymbol{x}_0| > a, \tag{4.13}$$

with

$$\boldsymbol{u} = \boldsymbol{U}, \quad \text{const}, \quad \text{for} \quad |\boldsymbol{x} - \boldsymbol{x}_0| = a$$

and $\boldsymbol{u} \to \boldsymbol{0}$ at spatial infinity, with the sphere centred at $\boldsymbol{x}_0$ at any given instant.

Noting linearity of Stokes' equations allows the superposition of solutions, to find the flow field for the translating sphere, consider

$$u_i = G_{ij}g_j + D_{ij}q_j,$$

which solves Stokes equation and decays at spatial infinity. Imposing the no-slip condition on the sphere boundary $r = a$ we have

$$U_i = \frac{g_i}{a} - \frac{q_i}{a^3} + \hat{x}_i\hat{x}_j \left[\frac{1}{a^3}g_j + \frac{3}{a^5}q_j \right].$$

Comparing coefficients, we have

$$\boldsymbol{q} = -\frac{a^2}{3}\boldsymbol{g} \quad \text{and hence} \quad \boldsymbol{g} = \frac{3}{4}a\boldsymbol{U} = \frac{1}{8\pi\mu}[6\pi a\mu\boldsymbol{U}],$$

giving the solution for the flow around a translating sphere.

This readily allows us to calculate the viscous drag exerted by the surrounding fluid on a translating sphere, which is known as Stokes drag. In particular the potential dipole does not contribute to the force (it is the limit of a linear combination of "equal but opposite" solutions, which thus do not exert a force prior to taking the limit, and hence do not exert a force after taking the limit).

Stokes Drag

Let $\sigma_{ij}^{Stk} = T_{ijp}^{Stk}m_p$ be the stress associated with Stokeslet solution 4.9. We thus have

$$\nabla_j\sigma_{ij}^{Stk} = m_p\nabla_jT_{ijp}^{Stk} = -m_i\delta(\boldsymbol{x} - \boldsymbol{x}_0).$$

The stress due to the Stokeslet contributions for the sphere solution is thus

$$\sigma_{ij}^{Sphere} = 8\pi\mu T_{ijp}^{Stk}g_p$$

and hence the total drag force, that is the force exerted by the fluid on the sphere, is

$$
\begin{aligned}
F_i &= \int_{Sphere} \sigma_{ij}^{Sphere}n_j\mathrm{d}S = \int_{Sphere} \nabla_j\sigma_{ij}^{Sphere}\mathrm{d}V \\
&= 8\pi\mu \int_{Sphere} g_p\nabla_jT_{ijk}^{Sphere}dV = -8\pi\mu \int_{Sphere} g_p\delta(\boldsymbol{x} - \boldsymbol{x}_0)dV = -8\pi\mu g_p.
\end{aligned}
$$

Hence the drag force is given by

$$\boldsymbol{F} = -6\pi\mu a\boldsymbol{U}. \tag{4.14}$$
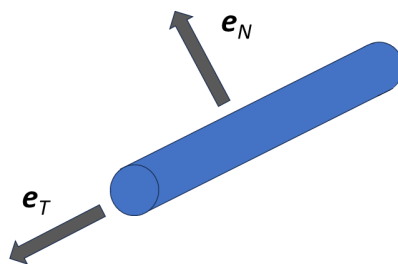
4.4.4 Resistive force theory

Figure 4.5: A small element of a slender filament, showing the tangential direction and a normal direction.

Foundation of resistive force theory

Consider a small element of a very slender filament of circular cross section, as in Fig. 4.5, moving in a viscous fluid. To provide the foundation for resistive force theory, our objective4.5 is to relate the drag force per unit length, $\boldsymbol{f}$ to the velocity of the filament, analogous to the relationship between the drag $\boldsymbol{F}$ and velocity $\boldsymbol{u}$ of a sphere in equation 4.14.

By the linearity of Stokes equations and symmetry of the circular cross section, the relation between drag per unit length and velocity must be of the form

$$\boldsymbol{f} = -C_N(\mathbf{I} - \boldsymbol{e}_T\boldsymbol{e}_T)\boldsymbol{U} - C_T(\boldsymbol{e}_T \cdot \boldsymbol{U})\boldsymbol{e}_T. \tag{4.15}$$

Thus our task reduces to finding C_T, C_N.

Resistive Force Theory *Definition.* Any theory of swimming that considers the mechanics of a beating ciliary or flagellar filament by using only the relationship between velocity and drag for isolated infinitesimal filament elements given by equation (4.15), is referred to as *resistive force theory*. Such theories often rely on the slenderness of the filament and always neglect possible non-local hydrodynamic interactions between different parts of the filament, for example if it turns back on itself.

Resistive Force Theory *Derivation.* To derive the relationship between drag and velocity for resistive force theory, consider a straight filament of length L and cross section radius a, with $a/L \ll 1$.

Suppose the filament is aligned along the x axis, between $x = 0$ and $x = L$, and is subject to a constant external force, uniformly distributed along its length, with force density per unit length $\boldsymbol{f}^{ext}$. We split the rod into $N = L/(2a) \gg 1$ elements of equal length, $2a$. Initially all hydrodynamic interactions of an element with its neighbours is neglected; the force each element exerts on the fluid is then $(L/N)\boldsymbol{f}^{ext}$.

Invoking linearity of Stokes equations, the speed of the αth element must be of the form

$$u_i^\alpha = \frac{L}{N}A_{ij}^\alpha f_j^{ext},$$

where the tensor $\mathbf{A}_{ij}^\alpha$ has $O(1)$ coefficients and, by the no slip boundary condition, u_i^α is also the speed of the fluid on the surface of the rod element. As all elements are equivalent the tensor A_{ij}^α in fact does not depend on α and we drop this superscript in the following.

To consider hydrodynamical interactions, at least approximately, we approximate each rod element by a Stokeslet, of strength $\boldsymbol{f}^{ext} L/N$, at locations

$$\boldsymbol{x}_0^\alpha = \left(\frac{L}{2N} + (\alpha - 1)\frac{N}{L}, 0, 0 \right), \quad \alpha \in \{1, ..., N\}.$$

This is equivalent to approximating each rod element as a sphere of diameter $2a = L/N$; the far field of such an object is dominated by the Stokeslet which decays like the inverse of distance; the potential dipole decays like the inverse of the cubed distance. Even at a distance of $2a$, ie. the centre of the next element, this approximation induces a relative error of about $2/2^3$, i.e. 25%, with improvements for more distant elements. Given the level of accuracy of resistive force theory, this is a tolerable error.

The flow induced by the αth stokeslet is

$$u_i^\alpha(\boldsymbol{x}) = \frac{1}{8\pi\mu}\frac{L}{N} G_{ij}(\boldsymbol{x}, \boldsymbol{x}_0^\alpha) f_j^{ext}.$$

Invoking linearity once more, the velocity at the βth segment is thus the linear superposition of the flow induced by the βth element and the flow induced by (our Stokeslet approximation of) all the other elements.

Hence, the flow at a point on the surface of the βth element, $\boldsymbol{x}^\beta \in \partial\Omega^\beta$, is

$$\begin{aligned}
u_i^\beta(\boldsymbol{x}^\beta) &= A_{ij}f_j^{ext}L/N + \sum_{\alpha;\ \alpha\neq\beta} \frac{L}{N} G_{ij}(\boldsymbol{x}^\beta, \boldsymbol{x}_0^\alpha) f_j^{ext} \\
&= A_{ij}f_j^{ext}L/N + \sum_{\alpha;\ \alpha\neq\beta} \frac{L}{8\pi\mu N} \left\{ \frac{\delta_{ij}}{r} + \frac{r_i r_j}{r^3} \right\} f_j^{ext}
\end{aligned}$$

where $\boldsymbol{r} = \boldsymbol{x}^\beta - \boldsymbol{x}_0^\alpha$, $r = |\boldsymbol{r}|$.

For $N \gg 1$ we approximate the sum by an integral, excluding a region around $\boldsymbol{x}^\beta$:

$$\begin{aligned}
u_i^\beta(\boldsymbol{x}^\beta) &\approx A_{ij}f_j^{ext}L/N + \frac{1}{8\pi\mu} \int_0^{s^\beta} ds \left\{ \frac{\delta_{ij}}{r} + \frac{r_i r_j}{r^3} \right\} f_j^{ext} \\
&+ \frac{1}{8\pi\mu} \int_{s^\beta+2a}^L ds \left\{ \frac{\delta_{ij}}{r} + \frac{r_i r_j}{r^3} \right\} f_j^{ext} + O(L/N)
\end{aligned}$$

where $s^\beta = (\beta - 1)L/N$ and $\boldsymbol{x}_0^\alpha \to s\boldsymbol{e}_x$ noting that $\boldsymbol{x}^\beta$ is still a fixed point on $\partial\Omega^\beta$. With the approximation $\boldsymbol{x}^\beta \approx (s^\beta + L/(2N))\boldsymbol{e}_x$ we have

$$\boldsymbol{r} = \boldsymbol{x}^\beta - \boldsymbol{x}_0^\alpha \approx \left(s^\beta + \frac{L}{2N} - s \right) \boldsymbol{e}_x,$$

and noting $L/[2N] = a$,

$$
\begin{aligned}
u_i^\beta &\approx A_{ij} f_j^{ext} L/N + \frac{1}{8\pi\mu} \left[\delta_{ij} + \delta_{i1}\delta_{j1}\right] f_j^{ext} \left[\int_0^{s^\beta} \frac{ds}{|s^\beta - s + a|} + \int_{2a+s^\beta}^L \frac{ds}{|s^\beta - s + a|} \right] \\
&\approx A_{ij} f_j^{ext} L/N \\
&+ \frac{1}{8\pi\mu} \left[\delta_{ij} + \delta_{i1}\delta_{j1}\right] f_j^{ext} \log\left(\frac{s^\beta(L - s^\beta)}{a^2}\right) \left(1 + O\left(\frac{a(L - 2s^\beta)}{s^\beta(L - s^\beta)} \frac{1}{\log\left(\frac{s^\beta(L-s^\beta)}{a^2}\right)}\right)\right).
\end{aligned}
$$

Considering away from the ends of the rod, so that $s^\beta = \gamma L$, with γ not close to zero or unity, so that $|\log(\gamma(1 - \gamma))| \sim O(1)$, we have

$$
u_i^\beta \approx A_{ij} f_j^{ext} L/N + \frac{1}{4\pi\mu} \left[\delta_{ij} + \delta_{i1}\delta_{j1}\right] f_j^{ext} \log\left(\frac{L}{a}\right) \left(1 + \frac{1}{2} \frac{\log(\gamma(1 - \gamma))}{\log\left(\frac{L}{a}\right)} + h.o.t.\right).
$$

Hence

$$
u_i^\beta \approx \frac{1}{4\pi\mu} \left[\delta_{ij} + \delta_{i1}\delta_{j1}\right] f_j^{ext} \log\left(\frac{L}{a}\right) \quad \text{as} \quad \frac{1}{N}, \ \frac{a}{L} \to 0,
$$

though extensive further work (eg matching into a prolate ellipsoid cap) is required to determine corrections at the ends.

A flagellum. Approximating a flagellum as a collection of slender straight elements, the velocity of the centre of each rod is related to the hydrodynamic force density exerted on the rod, at this level of approximation, by

$$
u_i \approx \frac{1}{4\pi\mu} \left[\delta_{ij} + \delta_{i1}\delta_{j1}\right] f_j^{ext} \log\left(\frac{L}{a}\right).
$$

Note this gives the velocity of a segment given the force per unit length applied on the fluid by the filament. We require the drag force per unit length, that is the force per unit length exerted on the filament by the fluid; this differs just by a minus sign (by Newton's third law).

The resistance coefficients, C_N, C_T

Hence, the hydrodynamic forces and velocities of elements of a flagellum are related by

$$
f_T = -C_T u_T, \quad f_N = -C_N u_N, \quad \text{where} \quad C_N = 2C_T = \frac{4\pi\mu}{\log\left(\frac{L}{a}\right)},
$$

with f_T, u_T, C_T denoting the force density, velocity and resistance coefficient in the tangential direction and f_N, u_N, C_N denoting the analogous quantities in the normal and binormal directions.

The original, more rigorous but harder, analysis can be found in [2], with further complexity if the careful higher order asymptotics of [3] are explored; therefore a cruder but simpler technique is presented here.

4.5   The cell swimming speed for small amplitude planar beating.
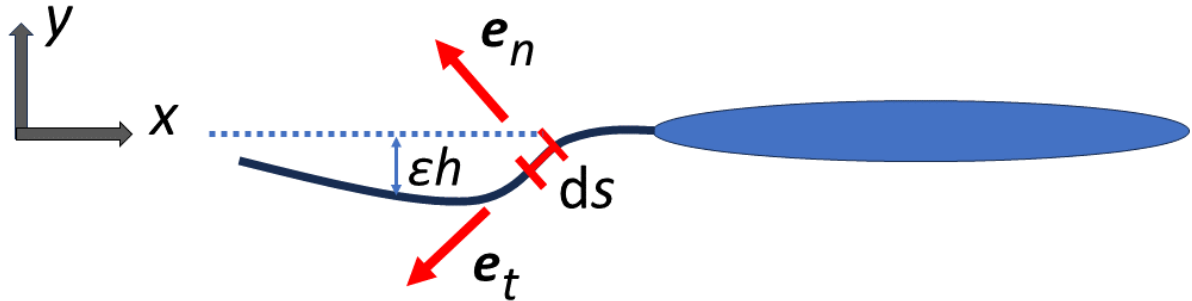

Figure 4.6: Motivated by *Leishmania major*, as in Fig. 4.2, we consider a swimming cell, with a slender cell body.

We consider a swimmer with a slender cell body with a planar flagellar beat, as schematically shown in Fig. 4.6 and motivated by *Leishmania major*, as in Fig. 4.2, though there is an interesting array of cell shape geometries in general.

Let $y = 0$ correspond to the midplane about which the flagellum beats, and let $y = \epsilon h(s,t)$ denote the location of the flagellum at time t and arclength s, with $s \in [0, L]$ where L is the flagellum length. We let a denote the flagellum radius and also assume a small amplitude beat so that $\epsilon \ll 1$.

We approximate the slender cell body by a cylindrical filament with no beating ($h = 0$) of radius a_b and length L_b. Thus the body resistance coefficients are

$$C_N^b = 2C_T^b = \frac{4\pi\mu}{\log\left(\dfrac{L_b}{a_b}\right)}.$$

Finally, in most expositions, it is assumed that the body has negligible velocity in the y direction, i.e. that the cell body velocity is $(U, 0)$ and that it does not rotate. Below we make this assumption, but it is generally unjustified and is explored further in the problem sheet.

Objective

Our objective is thus to find U, that is the swimming velocity along the x-axis, in terms of the flagellar beat $h(s,t)$.

Total force balance on the flagellum

- There is no net force on the cell.

- Hence

$$\mathbf{0} = (\text{Drag force on flagellum}) + (\text{Drag force on cell body}) \qquad (4.16)$$

We now use resistive force theory to determine the drag force on the flagellum in terms of $h(s, t)$ and then the drag force on the body. Projecting onto the x-axis will yield U, the swimming speed in the x direction, working to the leading non-trivial order in $\epsilon \ll 1$.

Flagellum

We have $\mathbf{e}_t = (-1, \epsilon h_s)$, $\mathbf{e}_n = (\epsilon h_s, 1)$ and the velocity of the flagellum element is given by $\mathbf{u} = (U, \epsilon h_t)$ noting cell body velocity in the y-direction is neglected. Hence the drag force per unit length on the element ds is given by

$$\mathbf{f} = -\left[C_N \mathbf{e}_n \cdot \mathbf{u} \mathbf{e}_n + C_T \mathbf{e}_t \cdot \mathbf{u} \mathbf{e}_t \right] = -\left[(C_N - C_T) \mathbf{e}_n \cdot \mathbf{u} \mathbf{e}_n + C_T \mathbf{u} \right]$$

and projecting this onto the x-direction we have

$$\begin{aligned}
\mathbf{f} \cdot \mathbf{e}_x &= -\left[(C_N - C_T) \mathbf{e}_n \cdot \mathbf{u} \mathbf{e}_n \cdot \mathbf{e}_x + C_T U \right] \\
&= -\left[(C_N - C_T)(\epsilon^2 h_s^2 U) + (C_N - C_T)(\epsilon^2 h_s h_t) + C_T U \right]
\end{aligned} \qquad (4.17)$$

Cell body

The calculation proceeds similarly only now we have a different geometry and thus different resistance coefficients C_N^b, C_T^b and $h = 0$. Hence, by trivial inheritance,

$$\mathbf{f}_b \cdot \mathbf{e}_x = -C_T^b U. \qquad (4.18)$$

Velocity

Combining equations (4.16), (4.17), (4.18)

$$0 = -C_T^b U L_b - \int_0^L \left[(C_N - C_T)\epsilon^2 h_s^2 U + (C_N - C_T)(\epsilon^2 h_s h_t) + C_T U \right] \mathrm{d}s \qquad (4.19)$$

Rearranging gives

$$\left[C_T^b L_b + (C_N - C_T)\epsilon^2 \int_0^L h_s^2 ds + C_T L \right] U = -(C_N - C_T)\epsilon^2 \int_0^L h_s h_t \mathrm{d}s.$$

Dropping the clearly subleading $O(\epsilon^2)$ term on the left-hand side immediately yields

$$U = \epsilon^2 \frac{C_T - C_N}{C_T^b L_b + C_T L} \int_0^L h_s h_t \mathrm{d}s = -\epsilon^2 \frac{1}{L + L_b C_T^b / C_T} \int_0^L h_s h_t \mathrm{d}s.$$

Brief exercise. How would the answer change if the cell had a spherical cell body of radius a?
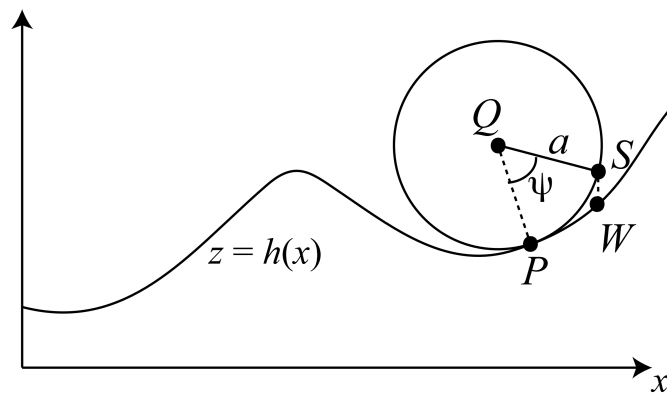
Appendix A

2D Curvature

Figure. Setup diagram for the determination of the curvature, $1/a$.

Important The normal, $\mathbf{n}$, is defined off surface by enforcing that it is independent of the direction perpendicular to the surface. As you will determine on the example sheet, this implies that

$$\nabla \cdot \mathbf{n} = \frac{d}{dx}\left(\frac{-h'}{(1+h'^2)^{1/2}}\right) = -\frac{h''}{(1+h'^2)^{3/2}}.$$

Without loss of generality the x coordinate of the point P is zero. Let

- Q be the centre of the best fit circle, of radius a to be determined
- S lie on the circle, and angle ψ from PQ.
- W lie on the curve $z = h(x)$ with the same x coordinate as S
- h_0, h'_0, h''_0 respectively denote $h(0)$, $h'(0)$ and $h''(0)$.
- $\mathbf{p}, \mathbf{q}, \mathbf{s}, \mathbf{w}$ denote the position vectors of P, Q, S, W
- $\mathbf{n}_0$, $\mathbf{t}_0$ denote the unit tangent and unit normal vectors at P.

- a be radius of the best fit circle; thus $1/a$ is the magnitude of the curvature.

We have

$$
\begin{aligned}
\mathbf{p} &= (0, h_0) \\
\mathbf{q} &= \mathbf{p} + a\mathbf{n}_0 \\
\mathbf{s} &= \mathbf{q} + a(\sin\psi \mathbf{t}_0 - \cos\psi \mathbf{n}_0) = (0, h_0) + a(1 - \cos\psi)\mathbf{n}_0 + a\sin\psi \mathbf{t}_0
\end{aligned}
$$

We require, for small x, that $\mathbf{s}, \mathbf{w}$ agree to $O(x^2)$ (and hence $O(\psi^2)$). We have

$$
\begin{aligned}
\mathbf{s} &= (0, h_0) + a(1 - \cos\psi)\mathbf{n}_0 + a\sin\psi \mathbf{t}_0 = (0, h_0) + a\psi^2 \mathbf{n}_0/2 + a\psi \mathbf{t}_0 + \dots \\
\mathbf{w} &= (x, h(x)) = (0, h_0) + (x, xh_0' + x^2 h_0''/2 + \dots)
\end{aligned}
$$

Thus we fix the circle radius a so that

$$
\frac{x}{a\psi}(1, h_0' + xh_0''/2) = \frac{\psi}{2}\mathbf{n}_0 + \mathbf{t}_0 = \frac{1}{(1 + h_0'^2)^{1/2}}\left(1 - \frac{\psi}{2}h_0', h_0' + \frac{\psi}{2}\right),
$$

on neglecting higher orders, i.e. terms that would not contribute to the expansion of $\mathbf{s}$ and $\mathbf{w}$ up to order $O(x^2), O(\psi^2)$. Comparing the first coefficient gives

$$
\frac{x}{a\psi} = \frac{1 - h_0'\psi/2}{(1 + h_0'^2)^{1/2}} \approx \frac{1}{(1 + h_0'^2)^{1/2}}\left(1 + O(\psi)\right).
$$

Comparing the second coefficient on use of the above gives

$$
\frac{h_0' + \psi/2}{(1 + h_0'^2)^{1/2}} = \frac{1 - h_0'\psi/2}{(1 + h_0'^2)^{1/2}}\left[h_0' + \frac{h_0''}{2}\left(\frac{x}{a\psi}\right)a\psi\right] = \frac{1 - h_0'\psi/2}{(1 + h_0'^2)^{1/2}}\left[h_0' + \frac{h_0''}{2}\frac{1}{(1 + h_0'^2)^{1/2}}(1 + O(\psi))a\psi\right]
$$

Hence, on neglecting higher orders,

$$
h_0' + \psi/2 = \left(1 - h_0'\frac{\psi}{2}\right)\left(h_0' + \frac{1}{2}\frac{a\psi h_0''}{(1 + h_0'^2)^{1/2}}\right) = h_0' + \frac{\psi}{2}\left(-h_0'^2 + \frac{ah_0''}{(1 + h_0'^2)^{1/2}}\right) + O(\psi^2).
$$

Terms at $O(\psi^0)$ automatically agree, while the next term, at $O(\psi)$, requires

$$
1 = -h_0'^2 + \frac{ah_0''}{(1 + h_0'^2)^{1/2}},
$$

i.e.

$$
\frac{1}{a} = \frac{h_0''}{(1 + h_0'^2)^{3/2}}.
$$

Thus the magnitude of the curvature at P is given by

$$
\frac{1}{a} = \frac{h_0''}{(1 + h_0'^2)^{3/2}} = -\nabla \cdot \mathbf{n}_0.
$$

More generally, the magnitude of the curvature at the point x is given by

$$\left| \frac{h''(x)}{(1 + h'(x)^2)^{3/2}} \right| = |\nabla \cdot \mathbf{n}|$$

and the curvature, κ, is *defined* by

$$\kappa = -\nabla \cdot \mathbf{n}.$$

Thus the curvature is positive if the centre of curvature lies above the surface and negative if it is below (with the contrast between above and below determined by the direction of the unit normal).

Bibliography

[1] J. R. Blake. Infinite models for ciliary propulsion. *J. Fluid Mech.*, 49:209–222, 1971.

[2] G. J. Hancock. The self-propulsion of microscopic organisms through liquids. *Proc. R. Soc. Lond. A*, 217:96–121, 1953.

[3] R. E. Johnson. An improved slender-body theory for Stokes-flow. *J. Fluid Mech.*, 99:411–431, 1980.

[4] C. Pozrikidis. *A Practical Guide to Boundary Element Methods with the Software Library BEMLIB*. CRC, 2002.